Volume 24
Number 5
4 February 2026
Pages 937-1144

Organic & Biomolecular Chemistry

rsc.li/obc

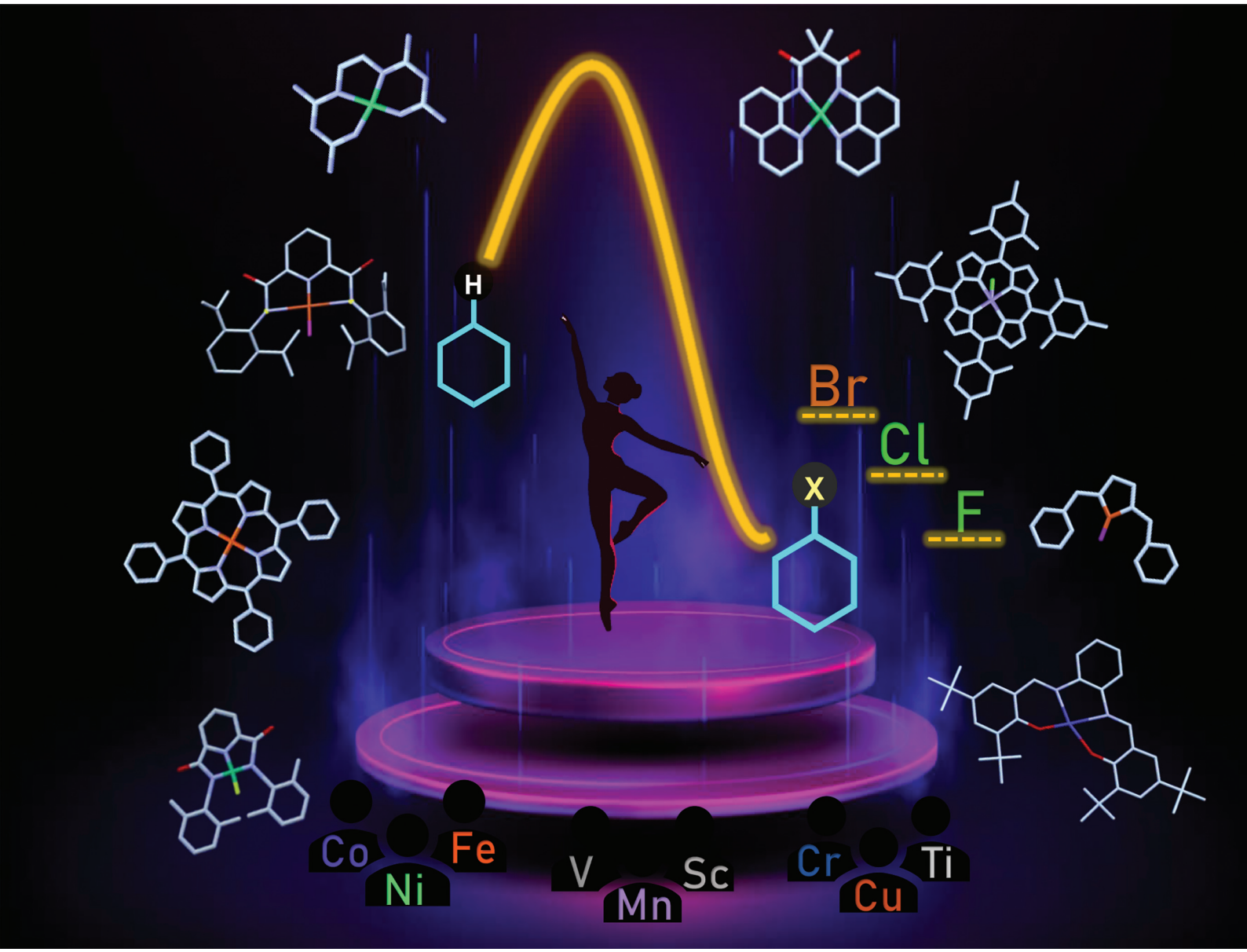

ISSN 1477-0520

ROYAL SOCIETY OF CHEMISTRY

REVIEW ARTICLE
Basab Bijayi Dhar *et al.*
C(sp^3)–H halogenation using first-row transition metal catalysts under homogeneous conditions

Organic & Biomolecular Chemistry

ROYAL SOCIETY OF CHEMISTRY

REVIEW

View Article Online
View Journal | View Issue

Open Access Article. Published on 14 November 2025. Downloaded on 3/15/2026 5:31:30 AM.
This article is licensed under a Creative Commons Attribution-NonCommercial 3.0 Unported Licence.

Check for updates

Cite this: *Org. Biomol. Chem.*, 2026, **24**, 946

C(sp^3)–H halogenation using first-row transition metal catalysts under homogeneous conditions

Monika,† Jaipriya Khatri,† Kritika Dogra, Rachana Choudhary, Sarban Kumar Yadav and Basab Bijayi Dhar *

Received 4th October 2025,
Accepted 10th November 2025

DOI: 10.1039/d5ob01584g

rsc.li/obc

The direct functionalization of unactivated C–H bonds has emerged as a promising strategy to achieve step-economical, atom-efficient, and environmentally benign chemical processes. In this context, ongoing research is focused on the design and development of biomimetic homogeneous catalysts based on first-row transition metals for C(sp^3)–H halogenation under mild conditions. In essence, this review highlights key advances in catalyst design based on first-row transition metals, showcasing their growing utility in the development of new synthetic methods.

1. Introduction

Halogenated organic compounds are essential in modern society (Fig. 1). Approximately 85% of pharmaceutical drugs involve chlorine or chlorinated compounds in their synthesis.[1a–c] The presence of carbon–halogen bonds in both synthetic active pharmaceutical ingredients and natural compounds enhances their stability, resistance to biodegradation and oxidation, biological activity, and membrane permeability. In the agrochemical sector, more than 90% of herbicides, fungicides, insecticides, acaricides, and nematicides produced since 2010 contain halogen atoms.[1a,d] For example, imidacloprid, a neonicotinoid used to control pests like sucking insects, soil insects, termites and fleas, is the most widely used insecticide globally.[2] To date, over 5000 naturally occurring organic halogenated compounds have been identified and characterized.[3] An example is vancomycin, a chlorine-containing antibiotic from *Streptomyces orientalis*, used to treat methicillin-resistant *Staphylococcus aureus* (MRSA) infections.[4] In 2021, marking the 50th anniversary of the National Cancer Act, the FDA approved six halogenated compounds, including tivozanib, sotorasib, melphalan flufenamide, asciminib, infigratinib, and umbralisib.[5] Fluorine is also widely used in

Department of Chemistry, School of Natural Sciences, Shiv Nadar Institution of Eminence Deemed to be University, Delhi NCR, Gautam Buddha Nagar, Dadri, UP-201314, India. E-mail: basabbijayi@gmail.com, basab.dhar@snu.edu.in
† Equal authorship.

Monika

Monika is currently a Ph.D. student and Senior Research Fellow (SRF) in the Department of Chemistry at Shiv Nadar Institution of Eminence (SNIoE), Delhi NCR. She completed her bachelor's and master's degrees at Panjab University, Chandigarh, before joining the research group of Dr Basab Bijayi Dhar. Her research focuses on the design and development of first-row transition metal complexes with amido-based ligand frameworks for organic transformations such as C–H hydroxylation, halogenation, and asymmetric halogenation, along with late-stage functionalization reactions, and electrochemical oxidation.

Jaipriya Khatri

Jaipriya Khatri joined the Chemistry Department at SNIoE, Delhi NCR, as a Ph.D. student in 2021. She joined the Catalysis Lab under the supervision of Dr Basab Bijayi Dhar after receiving her bachelor's and master's degrees from the University of Rajasthan. Her doctoral research focuses on the development of first-row transition metal-based homogeneous and heterogeneous catalysts for C–H activation and the electrochemical CO_2 reduction reaction ($ECCO_2RR$) in aqueous media.

This journal is © The Royal Society of Chemistry 2026

Open Access Article. Published on 14 November 2025. Downloaded on 3/15/2026 5:31:30 AM.
This article is licensed under a Creative Commons Attribution-NonCommercial 3.0 Unported Licence.

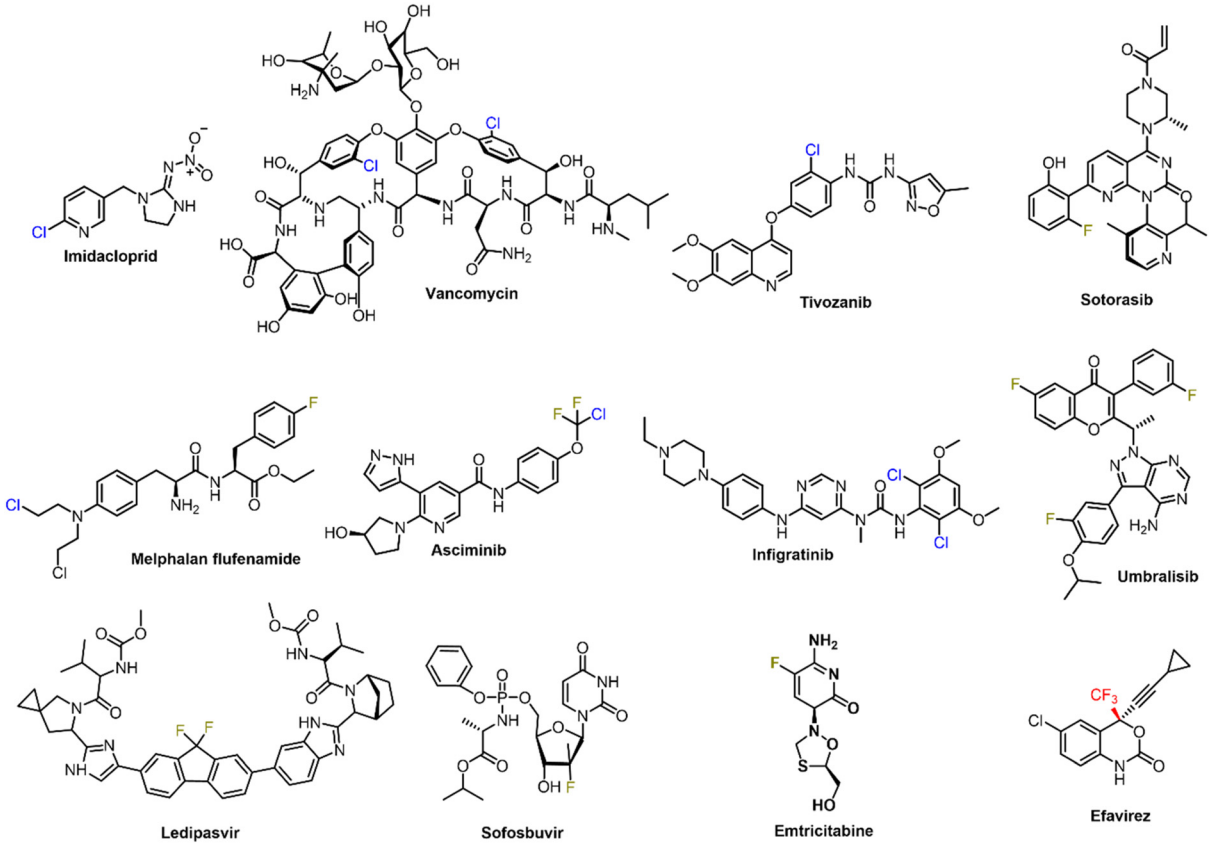

Fig. 1 Biologically important halogenated compounds.

modern medicinal chemistry.[6] Ledipasvir/sofosbuvir, a fluorinated drug marketed as Harvoni, is used to treat chronic hepatitis C.[7] In 2021, eight out of 14 newly approved drugs by the FDA contained fluorine.[8] Triple combination therapy is now the standard treatment for HIV infection, with one of the most successful combinations being Atripla, which contains two fluorinated drugs, such as emtricitabine and efavirenz, along with tenofovir.[9] Emtricitabine[10] and efavirenz[11] are nucleoside and non-nucleoside inhibitors of HIV-1 reverse transcriptase, the enzyme responsible for viral replication. In addition to these uses, various fluorinated and iodinated compounds are employed in radiotherapy and biomedical imaging.

From a synthetic chemistry standpoint, organohalides are typically produced by adding molecular halogens, hydrohalogenation, or using reagents that promote nucleophilic substitution and electrophilic aromatic substitution.[12] These methods can present environmental and selectivity challenges due to the reactive, toxic, and corrosive nature of the reagents

Kritika Dogra

Kritika Dogra is pursuing her PhD degree in the Department of Chemistry, SNIoE, Delhi-NCR, India. After obtaining her master's degree from Central University of Rajasthan, India, she joined the Catalysis Lab under the guidance of Dr Basab Bijayi Dhar. Her research focuses on catalyst design for various organic transformations, C–H activation, and electrochemical water oxidation.

Rachana Choudhary

Rachana Choudhary received her bachelor's degree from Banasthali University Rajasthan, and also obtained her master's degree in chemistry from the same university. She is currently pursuing her PhD under the supervision of Dr Basab Bijayi Dhar at SNIoE. Her research primarily focuses on photocatalyzed C–H activation and polymer degradation using first-row transition metal catalysts.

Open Access Article. Published on 14 November 2025. Downloaded on 3/15/2026 5:31:30 AM. This article is licensed under a Creative Commons Attribution-NonCommercial 3.0 Unported Licence.

involved, as well as the potential for creating complex mixtures of products. However, in nature, thousands of halogenated compounds are exclusively produced by specialised metalloenzymes, such as the Fe(II)/αKG-dependent enzyme SyrB2 [13] and heme- and vanadium-dependent haloperoxidases.[14] Flavin-dependent halogenases also show promise as biocatalysts for the regioselective halogenation of aromatic compounds.[15] Inspired by these natural enzymes, many research groups have explored various first-row transition metal complexes to activate inert C–H bonds. First-row transition metals are highly effective single-electron transfer (SET) agents, making them particularly well-suited for promoting radical-based C(sp^3)–H functionalization. In this review, we will report on the development of first-row transition metal catalysts for halogenation under homogeneous conditions, exploring their promising potential for enabling C–H activation and diversification in synthetic chemistry.

2. Enzymatic C–H halogenation

In nature, a range of enzymes are known to insert halogens into unactivated starting materials. Halohydrin dehalogenases (HHDHs), which have no transition metals, catalyse the reversible interconversion of epoxides into halohydrins.[16] Industrially, HHDHs are used in the production of chiral epichlorohydrin,[17] which serves as an intermediate in the manufacturing of synthetic rubbers, epoxy resins, paper chemicals, surfactants, adhesives, insecticides, agricultural chemicals, coatings, ion-exchange resins, solvents, plasticizers, and pharmaceuticals.[18] Additionally, it is a vital building block for biologically active compounds such as the β-adrenergic blocker (*S*)-atenolol and the amino acid derivative (*R*)-carnitine.[18] The most notable industrial use of HHDHs is in the synthesis of ethyl (*R*)-4-cyano-3-hydroxybutanoate, a critical precursor in the production of atorvastatin, the active ingredient in Lipitor®, which became the first drug to achieve annual sales exceeding 10 billion USD.[19]

The halogenation of an aliphatic methyl group on a protein-bound threonyl thioester is catalyzed by syringomycin halogenase (SyrB2), a non-heme Fe(II)/α-ketoglutarate (αKG)-dependent enzyme.[20] SyrB2 can also halogenate a non-native substrate, α-aminobutyric acid, to yield monochlorinated, dichlorinated, and trichlorinated products. It can also be used to broaden its reactivity scope to include multibromination.[21] The crystal structure reveals that the Fe centre is coordinated by two histidines, a bidentate αKG, water, and chloride (Fig. 1, species **1**).[22] Binding of L-Thr-S-SyrB1 would exclude water from the active site, enabling dioxygen binding (Fig. 2, species **2** and **3**). Decarboxylation of αKG generates a high-energy ferryl-oxo intermediate (Fig. 2, species **4**), which then abstracts a hydrogen atom from the substrate. The substrate radical subsequently captures the chlorine atom (Fig. 2, species **5**), producing chlorinated L-Thr-S-SyrB1 and regenerating the reduced Fe(II) center. Once the substrate carbon radical is formed, competition between chlorine ($Cl^{\bullet}$) and hydroxyl ($OH^{\bullet}$) transfer is expected. However, no threonine hydroxylation has been observed, indicating a strong preference for $Cl^{\bullet}$ rebound. It is important to note that SyrB2 requires substrates bound to a peptidyl carrier protein (PCP), which complicates its biotechnological application.

Haloperoxidases, which contain either heme iron or vanadium as a cofactor, halogenate electron-rich double bonds in substrates through the use of electrophilic halonium ions (Cl^+, Br^+ and I^+).[23] In both types of haloperoxidases, hypohalites formed in the enzyme active site diffuse out. As a result, any oxidative transformation is not influenced by the (chiral) enzyme environment, and the reaction's selectivity is determined by the reactivity of the starting material, not by the enzyme itself. The heme-dependent haloperoxidases generate

Sarban Kumar Yadav

Sarban Kumar Yadav obtained his Bachelor of Science (B.Sc.) degree in 2018 from the University of Burdwan and completed his Master of Science (M. Sc.) in Chemistry in 2020 from Bankura University. He is currently pursuing a Ph.D. degree under the supervision of Dr Basab Bijayi Dhar at SNIoE. His research is centered on inorganic chemistry, with a strong emphasis on homogeneous catalysis and organometallic chemistry. Currently he is designing various new ligands for asymmetric C–H halogenation.

Basab Bijayi Dhar

Dr Basab Bijayi Dhar earned his M.Sc. in Chemistry from the University of Calcutta and completed his Ph.D. at Jadavpur University under Prof. Rupendranath Banerjee on electron transfer reactions of manganese(IV). He did postdoctoral research with Prof. E. S. Gould (Kent State University) and Prof. R. Stan Brown (Queen's University). Currently he is an Associate Professor at SNIoE, Delhi NCR, and his research focuses on developing catalysts based on first-row transition metals for C–H activation, water oxidation, and CO_2 reduction, aiming to reduce dependence on rare metals in synthetic chemistry.

 This journal is © The Royal Society of Chemistry 2026

Open Access Article. Published on 14 November 2025. Downloaded on 3/15/2026 5:31:30 AM.
This article is licensed under a Creative Commons Attribution-NonCommercial 3.0 Unported Licence.

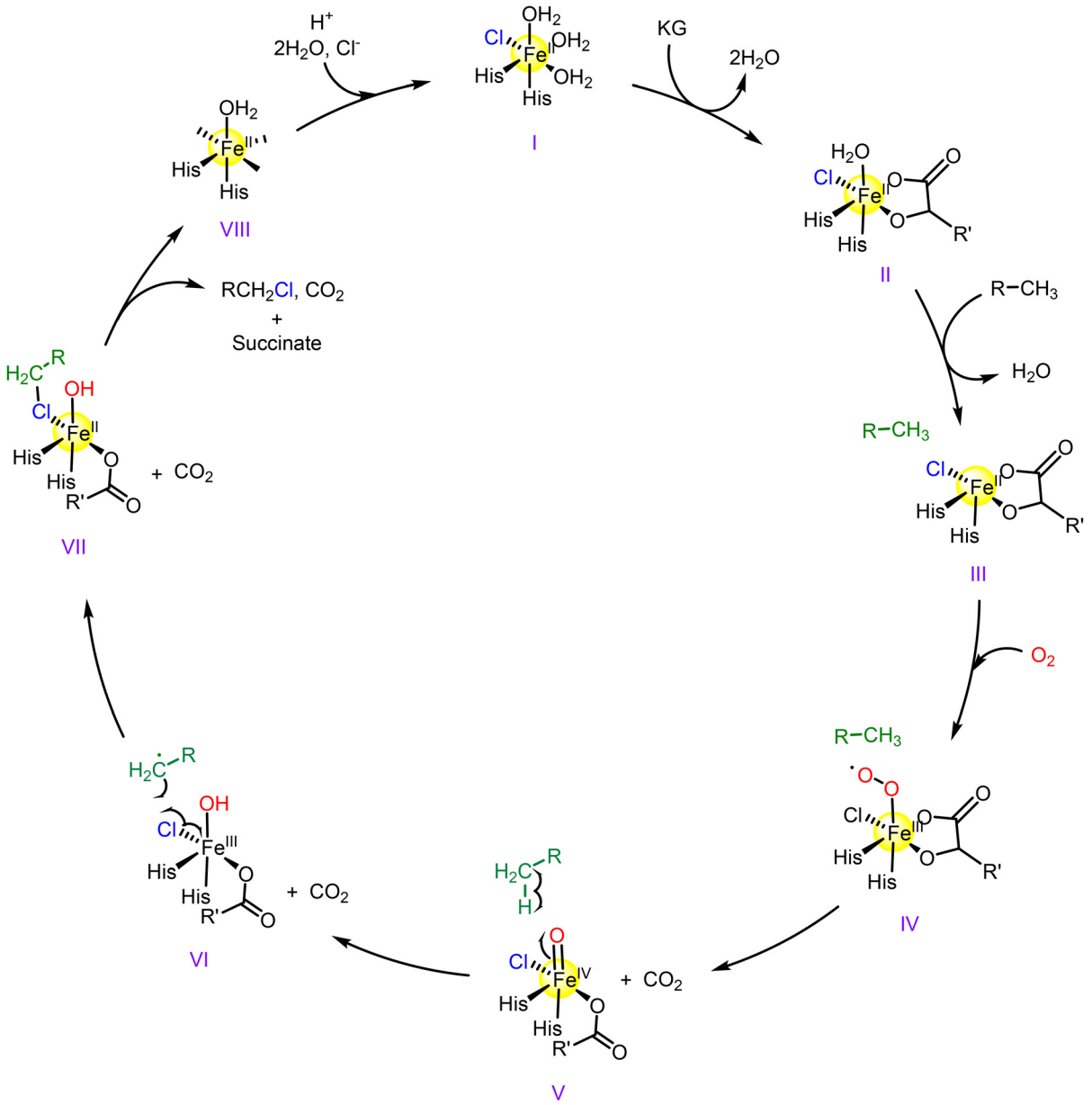

Fig. 2 Mechanistic pathway of SyrB2.

an Fe^{IV}-(oxo)-porphyrin$^{\bullet+}$ complex in the presence of hydrogen peroxide (H_2O_2), which then oxidizes halides (Fig. 3).[24a] The research group of Holtmann utilized the heme-dependent LfCPO for halogenating the terpene thymol to enhance its antimicrobial properties.[25] Itoh *et al.* studied the halogenation of various electron-rich arenes using CpVBPO from *Corallina pilulifera*[26a] and halohydroxylation of alkenes (Fig. 4) using LfCPO62.[26b] When these reactions were carried out in aqueous media in the presence of OH^- ions, the formation of halohydrins took place.

The vanadium-dependent haloperoxidases use a peroxovanadate species formed by the reaction with H_2O_2 (Fig. 4).[24b] Schrader and his team explored the halohydroxylation reactions of terpenes using chloroperoxidase from *Caldariomyces fumago*.[24c,d] Chemoenzymatic production of halogenated phenolic monoterpenes thymol and carvacrol using chloroperoxidase extracted from *Caldariomyces fumago* was reported by Getrey *et al.*[27] In a similar manner, Hartung and co-workers investigated the bromination of various phenols using the vanadium-dependent bromoperoxidase extracted from *Ascophyllum nodosum*.[28] Using vanadium-dependent chloroperoxidase from *Curvularia inaequalis*, the efficient bromination of thymol (TON ~2 000 000) was carried out by Fernández-Fueyo *et al.*[29]

Recently, flavin-dependent non-metal tryptophan halogenases have become popular for synthetic applications.[30] These enzymes regioselectively chlorinate electron-rich carbon centres using electrophilic halonium ions (Fig. 5). Members of

Open Access Article. Published on 14 November 2025. Downloaded on 3/15/2026 5:31:30 AM.
This article is licensed under a Creative Commons Attribution-NonCommercial 3.0 Unported Licence.

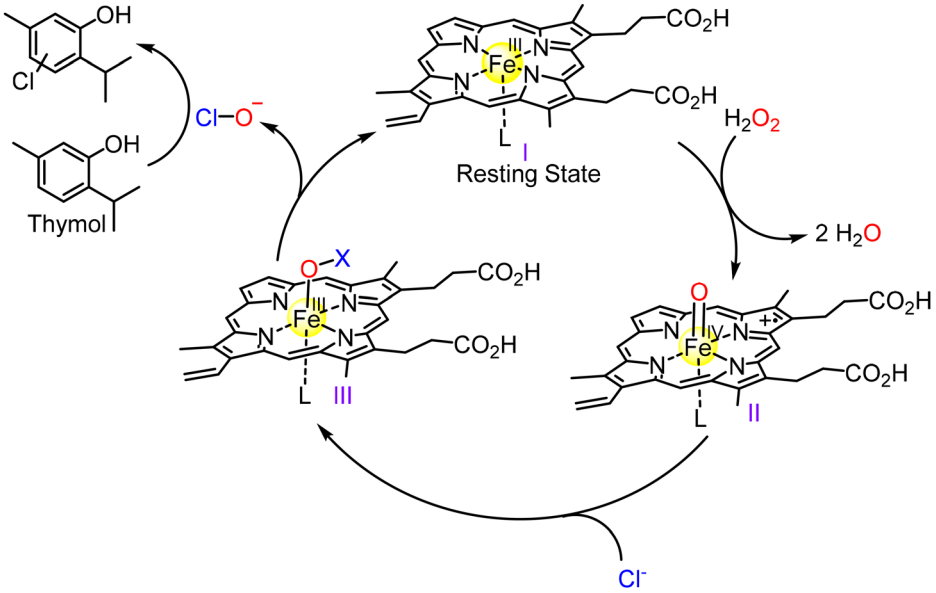

Fig. 3 Mechanistic pathway of heme-dependent haloperoxidase and chemoenzymatic halogenation of thymol by Holtmann and his research group.

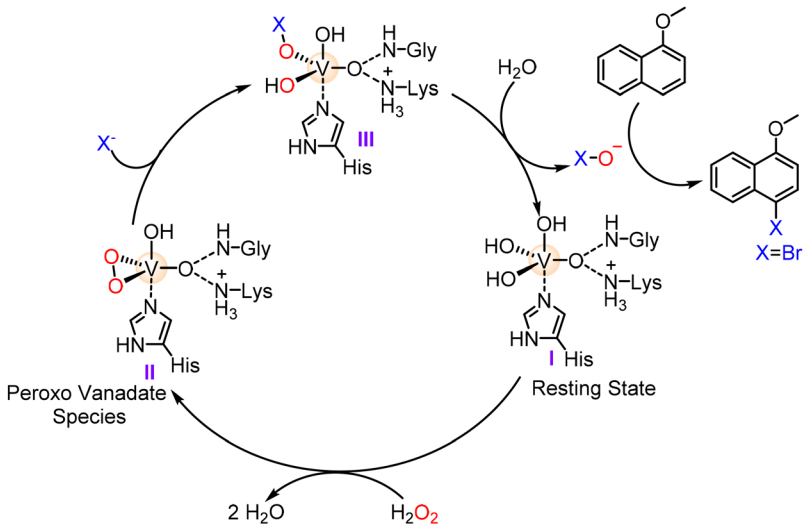

Fig. 4 Bromination of activated arenes using the vanadium-dependent bromoperoxidase.

this halogenase superfamily have been identified in the biosynthetic pathways of the antibiotics balhimycin and vancomycin, the antitumor agent rebeccamycin, and other halometabolites. Likely, regiospecific halogenation reactions carried out by bacteria are largely catalysed by flavin-dependent halogenases. To account for the regioselectivity, two mechanisms have been proposed. On one hand, the substrate is oxidized to an epoxide, which is decomposed by a nucleophilic attack of Cl^-. On the other hand, direct chlorination by a high-energy flavin hypochlorite intermediate occurs. Van Pèe and coworkers revealed regioselective halogenation of the indole moiety using various flavin-dependent tryptophan halogenases under benign conditions (X: Cl, Br).[31]

3. C–H chlorination and bromination

3.1 Non-heme iron-based catalysts

Gif chemistry, originally developed by Sir Derek Barton for the selective functionalization of saturated hydrocarbons, has evolved beyond its initial focus on oxidation to encompass halogenation reactions.[32,33] The $GoAgg^{III}$ system, an advanced variant of Gif chemistry, has demonstrated effective bromination of alkanes using polyhaloalkanes such as $CBrCl_3$ as halogen sources.[33a] Reaction rates vary with the structure of the polyhaloalkane used, and the selectivity toward various saturated hydrocarbons differs markedly from that seen in radical halogenation. Furthermore, product distribution

 This journal is © The Royal Society of Chemistry 2026

Open Access Article. Published on 14 November 2025. Downloaded on 3/15/2026 5:31:30 AM.
This article is licensed under a Creative Commons Attribution-NonCommercial 3.0 Unported Licence.

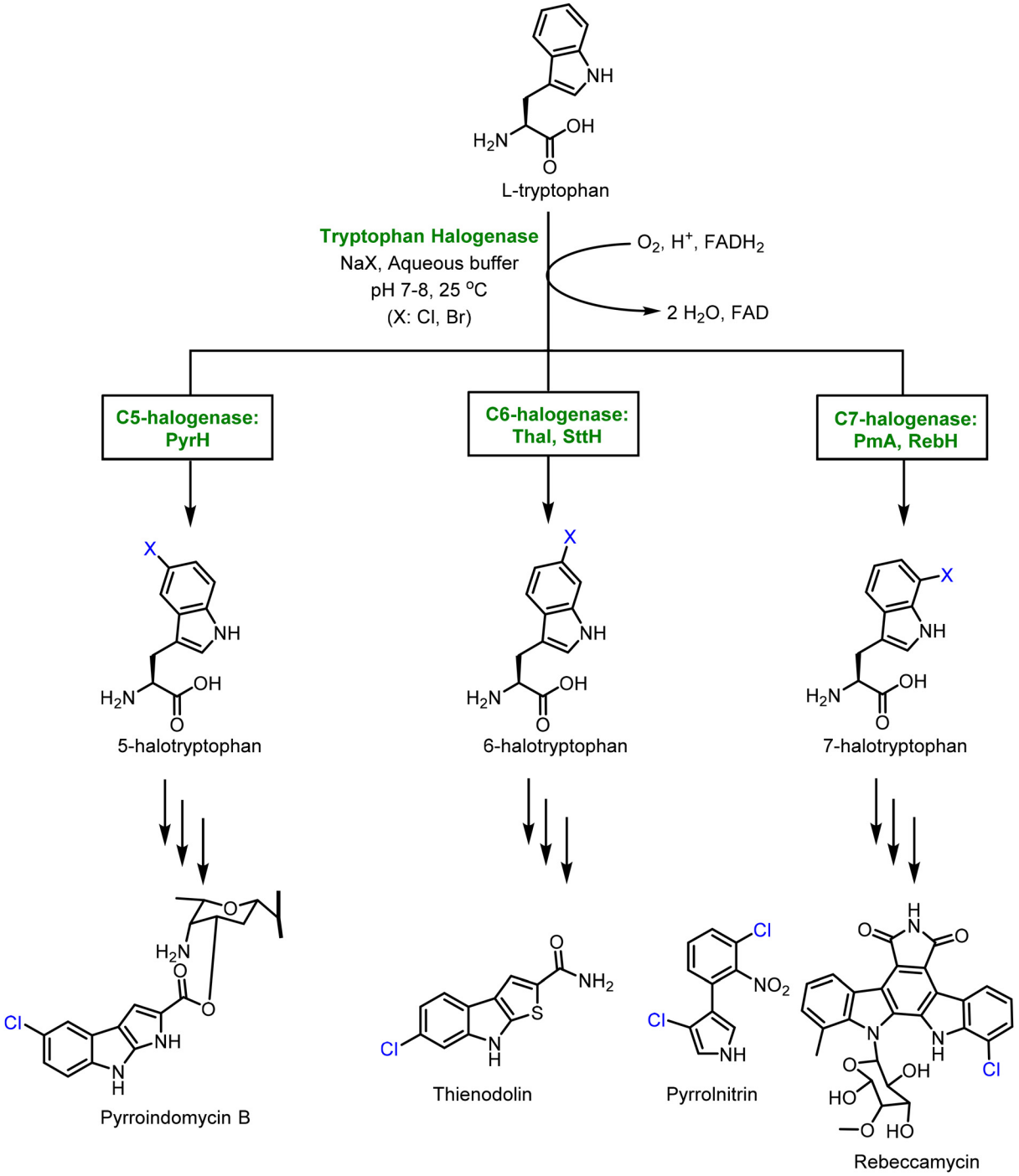

Fig. 5 Flavin-dependent non-metal tryptophan halogenases and biosynthetic pathways of the antibiotics balhimycin and vancomycin, the antitumor agent rebeccamycin, and other halometabolites using tryptophan halogenases.

studies, such as those involving the bromination of cyclohexyl bromide, highlight a distinct regioselectivity profile under Gif-type conditions. This selectivity is attributed to the involvement of a high-valent metal-oxo intermediate rather than a simple, unselective free radical. The metal center directs the hydrogen abstraction, preferring the less sterically hindered secondary position.[32] However, isolating the highly reactive, short-lived metal intermediates in Gif chemistry has been a significant challenge. Therefore, the nature of the reaction mechanism, whether radical or non-radical, was highly debated and described as the "Gif paradox".[33b] Chlorination reactions using similar systems (*e.g.*, GoAgg^{III}) and chlorine-containing reagents have also been explored, further underscoring the generality of Gif-type halogenation for forming

Open Access Article. Published on 14 November 2025. Downloaded on 3/15/2026 5:31:30 AM.
This article is licensed under a Creative Commons Attribution-NonCommercial 3.0 Unported Licence.

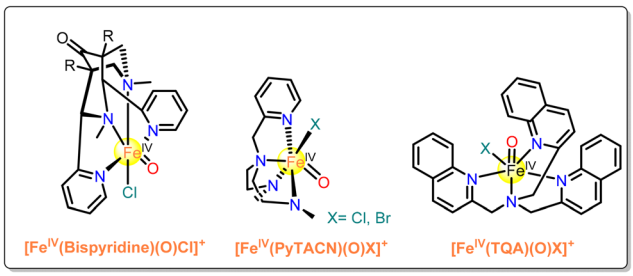

Fig. 6 Biomimetic iron-oxo-halide frameworks for enzyme-inspired halogenation.

both C–Br and C–Cl bonds.[33a] In summary, while Barton's Gif chemistry opened a novel pathway for C–H functionalization under non-radical conditions, its practical limitations include environmental concerns, selectivity issues, and poor scalability, highlighting the need for more refined, catalytic, and sustainable halogenation methods.

In 1993, Que Jr. and co-workers reported a biomimetic system that models the activity of non-heme halogenases.[34a] They synthesized a series of $[Fe(III)X_2]^+$ complexes (X = Cl, Br, N_3), where L is tris(2-pyridylmethyl)amine (TPA), capable of functionalizing alkanes under ambient conditions. Upon treatment with a stoichiometric amount of alkyl hydroperoxide in the presence of cyclohexane, these non-heme iron complexes generated halocyclohexane in good yields. A significant kinetic

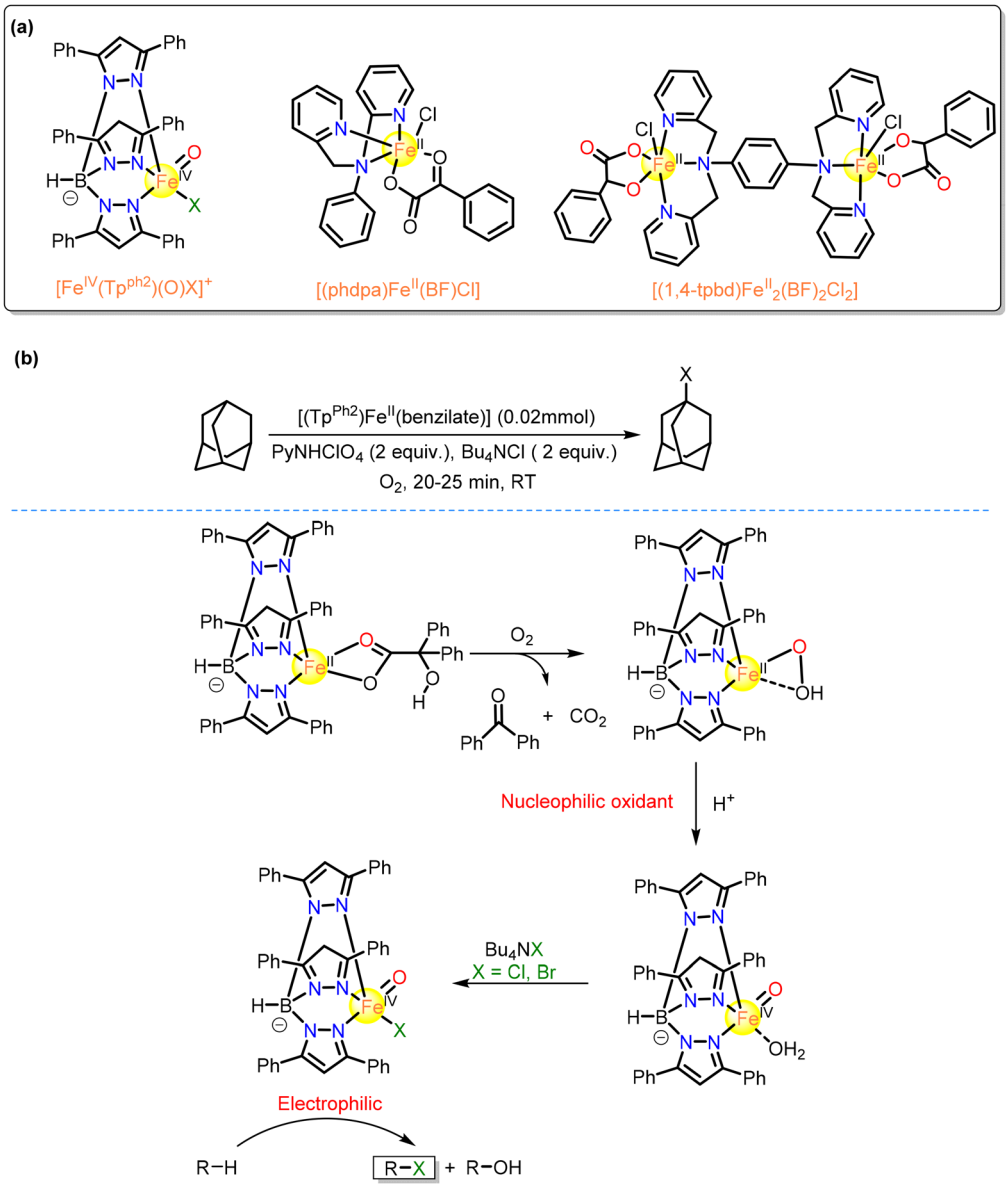

Fig. 7 (a) Various Fe-based non-heme complexes utilized in C–H halogenation. (b) Proposed mechanistic pathway for the generation of an electrophilic iron-oxo species and its involvement in aliphatic C–H halogenation.

Open Access Article. Published on 14 November 2025. Downloaded on 3/15/2026 5:31:30 AM. This article is licensed under a Creative Commons Attribution-NonCommercial 3.0 Unported Licence.

isotope effect (KIE) was observed when comparing reactions using cyclohexane and [D_{12}]cyclohexane (K_H/K_D = 7–10), indicating that hydrogen atom abstraction (HAA) constitutes the rate-determining step of the transformation. Notably, the magnitude of the KIE was found to vary depending on both the halide ligand and the structure of the tripodal ligand framework. In contrast, changing the nature of the peracid oxidant, by altering the R group (*e.g.*, *tert*-butyl or cumyl), had no measurable impact on the reaction outcome. The authors proposed the involvement of an iron(III)-alkyl peroxide intermediate, which undergoes O–O bond cleavage to generate a high-valent iron(V)-oxo-halide species. This highly reactive intermediate is responsible for the hydrogen atom abstraction (HAA) from the C–H bonds of cycloalkanes. The alkyl radical then undergoes a halide rebound pathway, predominantly yielding the halogenated product, with only a minor amount of the hydroxylated product observed. However, Arends *et al.* proposed that in the $[Fe(TPA)X_2]^+$/*t*-BuOOH system (X = Cl, Br *etc.*), *t*-BuO$^\bullet$ radicals, rather than metal-based oxidants, serve as the sole agents responsible for alkyl radical generation.[34b] The preferential formation of the halogenated compound is attributed to the difference in redox potentials between the chloride and hydroxide radicals during the radical rebound step, with E° ($Cl^\bullet/Cl^-$) = 0.36 V *vs.* NHE and E°($OH^\bullet/OH^-$) = 2.20 V *vs.* NHE. However, in the presence of excess alkyl hydroperoxide (150 equivalents with respect to the Fe catalyst), cyclohexanol was the predominant product, which is the major drawback of the $[Fe(TPA)X_2]^+$/*t*-BuOOH system. Noack and Siegbahn investigated the mechanism of oxidative chlorination catalyzed by the non-heme iron complex $[(TPA)Fe^{III}Cl_2]^+$ in the presence of

Table 1 Comparison of different reported homogeneous catalysts for C–H bond chlorination of cyclohexane

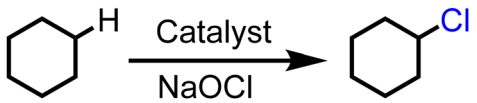

S. no.	Catalyst	TON (chlorination of cyclohexane)
1	Mn(TPP)Cl/NaOCl[43]	87
2	$[Ni^{II}(Pytacn)(CF_3SO_3)_2]$ (Pytacn = 1-(2-pyridylmethyl)-4,7-dimethyl-1,4,7-triazacyclononane)/NaOCl[44]	24
3	$[Ni^{II}(L)]$ (L = bisamidate ligand)/NaOCl[45]	44
4	$[Fe^{IV}(2\ PyN2Q)(O)]^{2+}$/NaOCl[40b]	52
5	$[Ni^{II}$-amidoquinoline]/NaOCl[46a]	212
6	$[Ni^{II}$-bisbiguanide]/NaOCl[47]	680

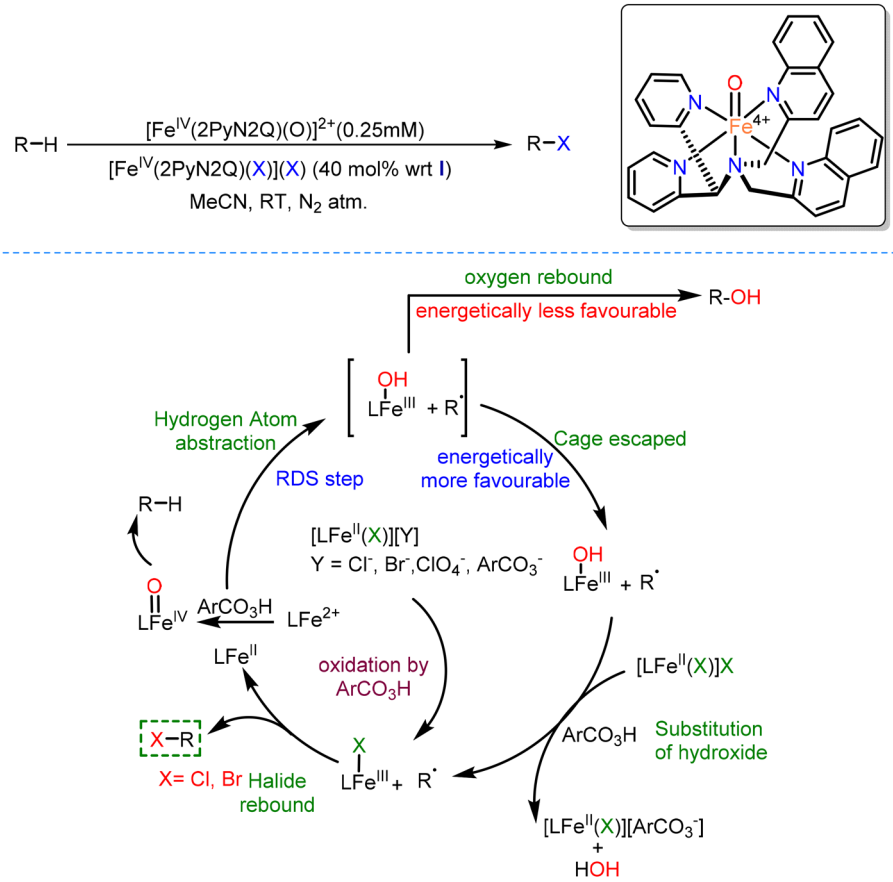

Fig. 8 Plausible mechanistic pathway for C–H halogenation mediated by iron(IV)-oxo in the presence of iron(II)-halide complexes.

Open Access Article. Published on 14 November 2025. Downloaded on 3/15/2026 5:31:30 AM.
This article is licensed under a Creative Commons Attribution-NonCommercial 3.0 Unported Licence.

a peroxide oxidant using density functional theory (DFT) calculations.[35] They reported that $Fe^{V}{=}O$ or $Fe^{IV}{=}O$ species serve as the key catalytic intermediate.

In 2010, Comba and co-workers reported a dichloroiron(II) complex featuring a tetradentate bispidine ligand {L = 3,7-dimethyl-9-oxo-2,4-bis(2-pyridyl)-3,7-diazabicyclo[3.3.1]nonane-1,5-dicarboxylate methyl ester} (Fig. 6), which demonstrated catalytic activity for C–H halogenation of alkanes using various oxidants, including PhIO, TBHP, and H_2O_2.[36] The selectivity between halogenation and hydroxylation was found to be

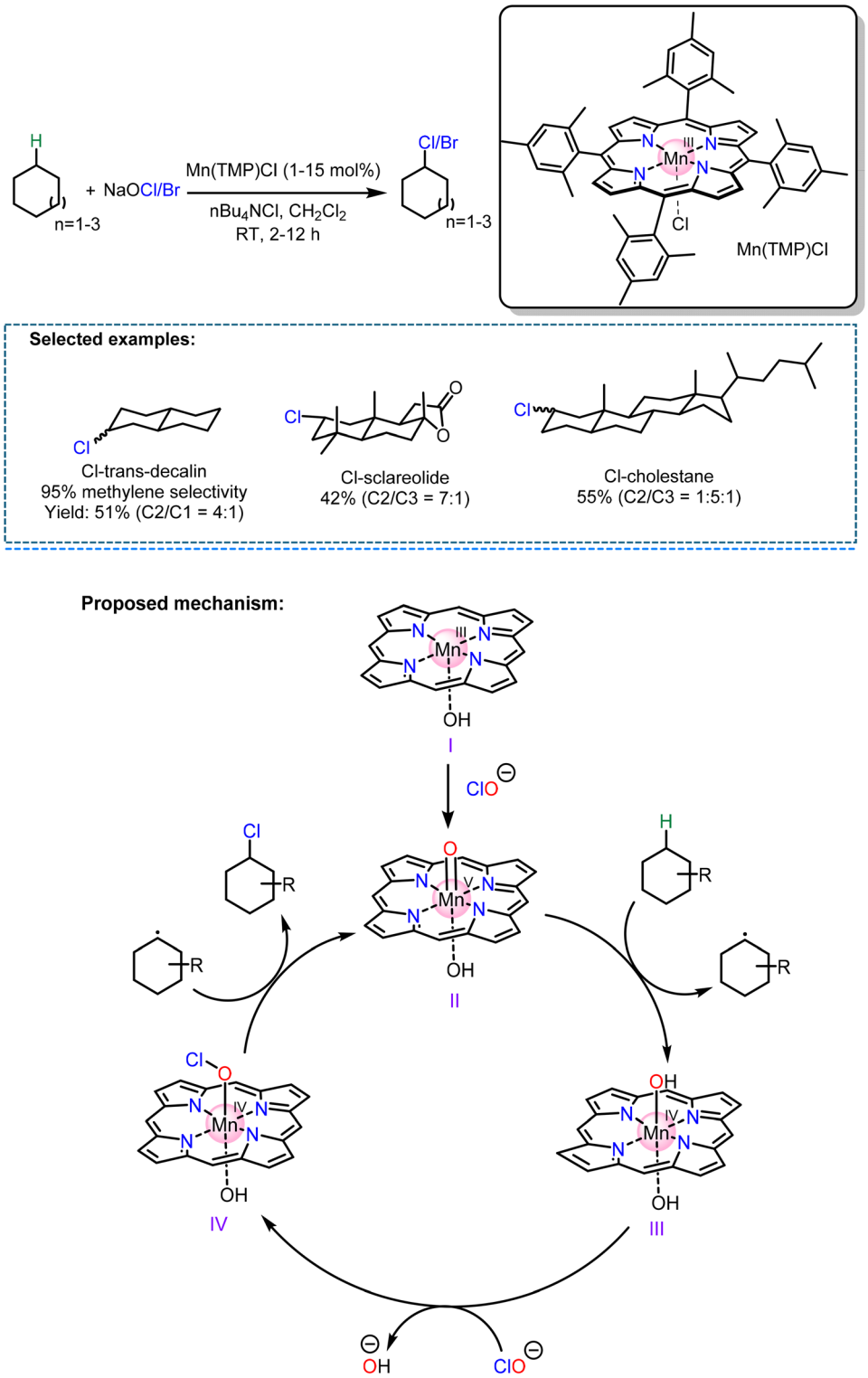

Fig. 9 Groves' catalyst for C–H chlorination and bromination.

Open Access Article. Published on 14 November 2025. Downloaded on 3/15/2026 5:31:30 AM.
This article is licensed under a Creative Commons Attribution-NonCommercial 3.0 Unported Licence.

oxidant-dependent. Kinetic isotope effect (KIE) studies using cyclohexane and [D_{12}]cyclohexane revealed K_H/K_D values of 14 (PhIO), 9 (TBHP), and 3 (H_2O_2), indicating that hydrogen atom abstraction (HAA) is the rate-determining step and suggesting the involvement of different high-valent iron-oxo intermediates, either Fe^{V}=O or Fe^{IV}=O, depending on the oxidant. Subsequently, Costas and co-workers explored the reactivity of $[Fe^{IV}(PyTACN)(O)Cl]^+$ (Fig. 6) for C–H halogenation.[37] However, no halogenated products were observed due to the strong coordination of the halide to the metal center, which likely inhibits halogen rebound. Later, Que and co-workers reported the $[Fe^{IV}(O)(TQA)X]^+$ (X = Cl, Br) complex (Fig. 6), where TQA = tris (quinolin-2-ylmethyl)amine, as an effective system for C–H bond halogenation.[38] This complex represents the first synthetic example that reproduces the Mössbauer parameters characteristic of an $S = 2$ oxoiron(IV) species.

Paine and co-workers reported the first example of a biomimetic iron(II) complex supported by the hydro[tris(3,5-diphenyl-pyrazol-1-yl)]borate ligand (Fig. 7), which undergoes aerobic oxidation under acidic conditions.[39a] This system enables aliphatic C–H bond halogenation of substrates such as adamantane, toluene, and cyclohexane *via* the formation of an Fe(IV)-oxoaquo intermediate (Fig. 7) in the presence of tetra-*n*-butylammonium halide and pyridinium perchlorate. The same group also developed two non-heme iron(II)-α-keto acid complexes: [(phdpa)Fe(BF)Cl] and [(1,4-tpbd)$Fe_2(BF)_2Cl_2$] (Fig. 7), incorporating phdpa (*N*,*N*-bis(2-pyridylmethyl)benzene-1,4-diamine), BF (benzoylformate), and 1,4-tpbd (*N*,*N*,*N*′,*N*′-tetrakis (2-pyridylmethyl)benzene-1,4-diamine) as ligands.[39b] These systems catalyze the oxidative halogenation of aliphatic C–H bonds using molecular oxygen as the terminal oxidant. Alongside halogenated products, hydroxylated and overoxidized species were also observed.

Maiti and co-workers developed a new synthetic scheme for selective halogenation utilizing a pentadentate ligand [ligand (1,1-di-(pyridin-2-yl)-*N*,*N*-bis(quinolin-2-yl-methyl)methanamine), 2PyNQ]-derived nonheme iron complex.[40a] They used a combination of $[Fe^{IV}(2PyN_2Q)(O)]^{2+}$ and $[Fe^{II}(2PyN_2Q)(OTf)_2]$, where Fe^{IV}=O abstracts the hydrogen from the aliphatic substrate *via* hydrogen atom abstraction (HAA) to form the radical, and iron(II)-halide used as the halide source to generate the halogenated product (Table 1 and Fig. 8).[40b] Maiti's research

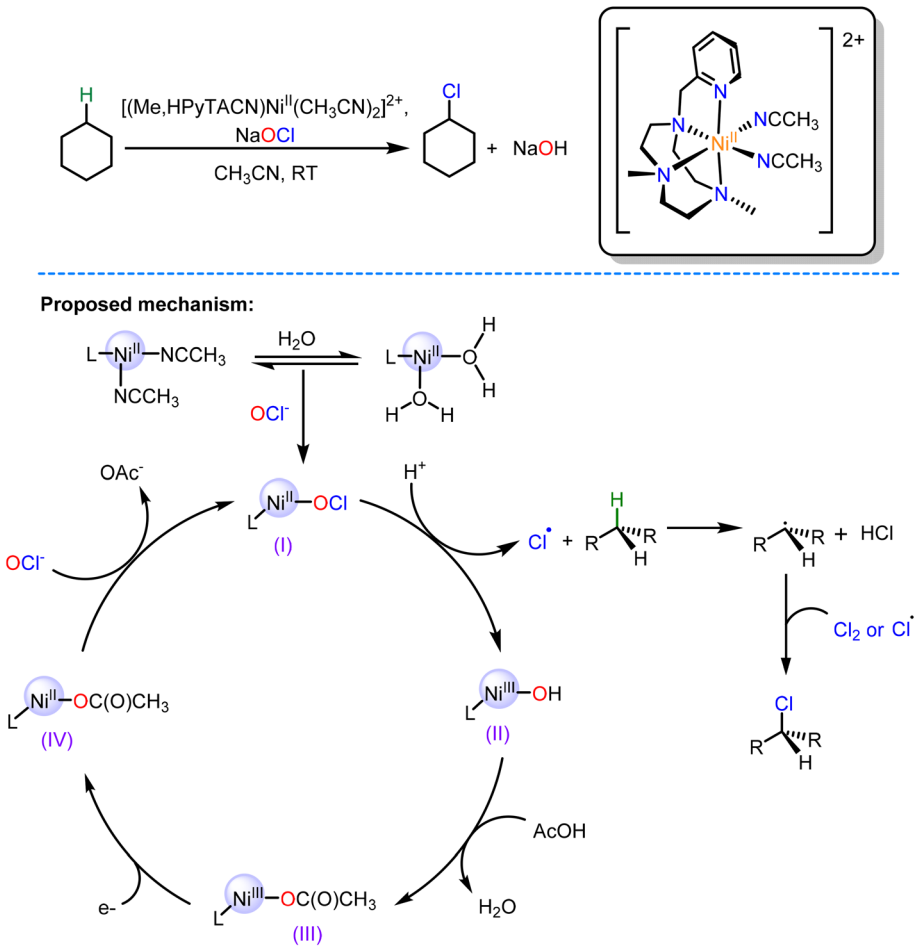

Fig. 10 Costa's catalyst for the chlorination of alkanes.

Open Access Article. Published on 14 November 2025. Downloaded on 3/15/2026 5:31:30 AM.
This article is licensed under a Creative Commons Attribution-NonCommercial 3.0 Unported Licence.

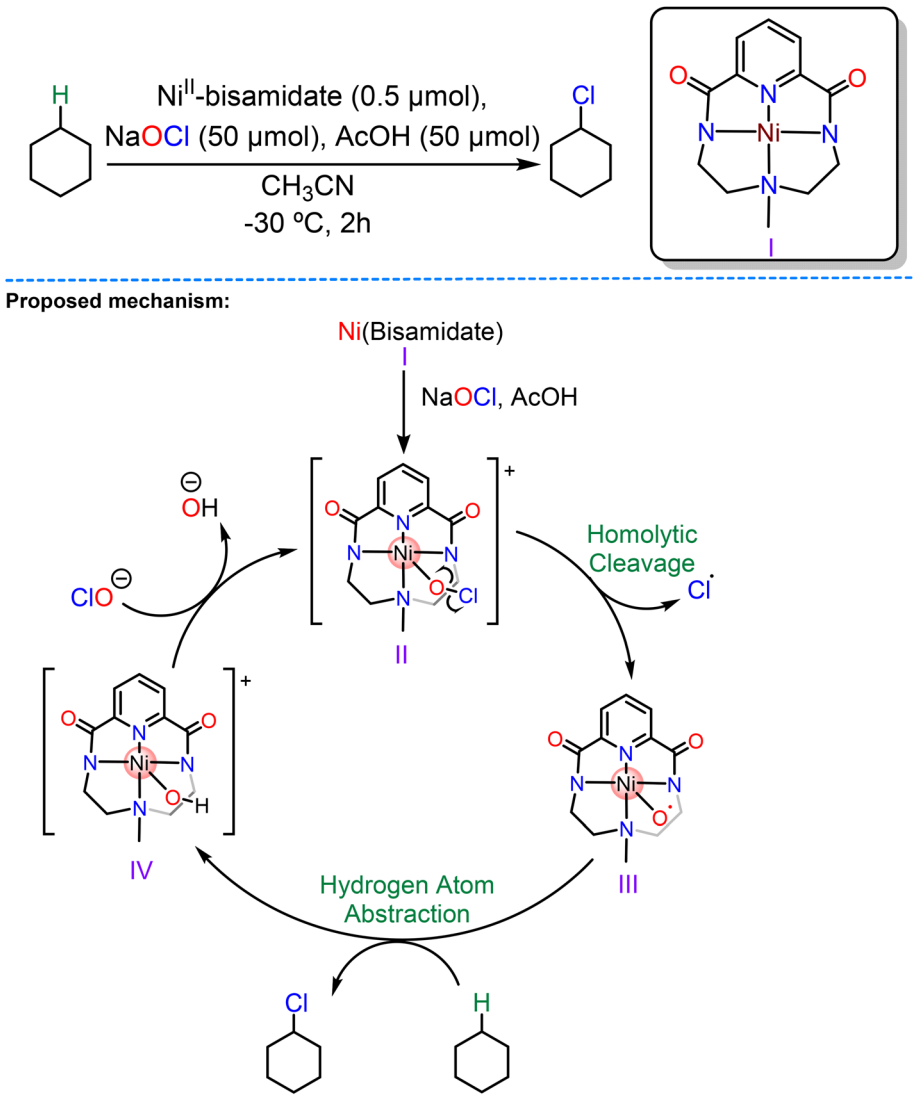

Fig. 11 A. Company's catalyst for the chlorination of alkanes.

Table 2 Comparison of catalytic C–H chlorination and bromination of different substrates[46a,47]

S. no.	Substrate	Product	TON (Ni^{II}-amidoquinoline)[a]	TON (Ni^{II}-bisbiguanide)[b]
1	Cyclohexane	Chlorocyclohexane	212	680 ± 60
2	Methylbenzene	(Chloromethyl)benzene	202	200 ± 20
3	Ethylbenzene	(1-Chloroethyl)benzene	208	370 ± 30
4	Adamantane	1-Chloroadamantane (3°)	173	1600 ± 200 (3°)
		2-Chloroadamantane (2°)	5	320 ± 30 (2°)
5	Methylbiphenyl	4-Chloromethylbiphenyl	196	260 ± 25
6	2,3-Dimethylbutane	2-Chloro-2,3-dimethylbutane	92	130 ± 20
7	*n*-Hexane	2°-Chlorohexane	—	108 (2°)
		1°-Chlorohexane		27 (1°)
8[c]	Cyclohexane	Bromocyclohexane	—	125
9[c]	Methylbenzene	(Bromomethyl)benzene	—	82
10[c]	Ethylbenzene	(1-Bromoethyl)benzene	—	115 (2°); 6 (1°)

[a] Reaction conditions: Ni catalyst (0.25 mmol), substrate (0.25 mmol), NaOCl (0.25 mmol), and AcOH (0.25 mmol) in 1 mL of CH_2Cl_2/CH_3CN (2 : 8 v/v) at RT for 30 minutes under N_2. [b] Ni catalyst (0.05 μmol), substrate (0.25 mmol), NaOCl (0.30 mmol), and AcOH (0.15 mmol) in 1 mL of H_2O:$CHCl_3$ (7 : 3 v/v) for 30 minutes at RT. [c] Ni catalyst (0.05 μmol), substrate (0.25 mmol), NaOCl (0.30 mmol), NaBr (0.30 mmol), and AcOH (0.15 mmol) in 1 mL of $H_2O/CHCl_3$ (7 : 3 v/v) for 30 minutes at RT. The products were identified using GC-MS.

Open Access Article. Published on 14 November 2025. Downloaded on 3/15/2026 5:31:30 AM.
This article is licensed under a Creative Commons Attribution-NonCommercial 3.0 Unported Licence.

group has also demonstrated a method for benzylic C–H chlorination using an easily prepared Mn(salen) complex as the catalyst in the presence of NaOCl.[40c]

Han and co-workers have developed a bioinspired pincer iron(III) complex that catalyzes both the oxidation and chlorination of aliphatic C(sp^3)–H bonds. The use of *cis*-decalin as a mechanistic probe suggests the involvement of a long-lived carbon-centered radical intermediate, indicative of a stepwise reaction pathway. Detailed studies point to an iron-oxo species as the likely oxidant responsible for the rate-determining C–H activation step.[41] Recent investigations by the research groups of Company and Costas have explored the reactivity of a series of well-defined iron(IV)-oxo complexes supported by variants of the tetradentate 1-(2-pyridylmethyl)-1,4,7-triazacyclononane (Pytacn) ligand.[42] These studies revealed a remarkable switch in chemoselectivity during C–H bond functionalization, modulated by the reaction conditions. In the presence of halide anions, the complexes promote exclusive C–H oxygenation, whereas the addition of a superacid diverts the reaction pathway towards C–H halogenation. Mechanistic investigations

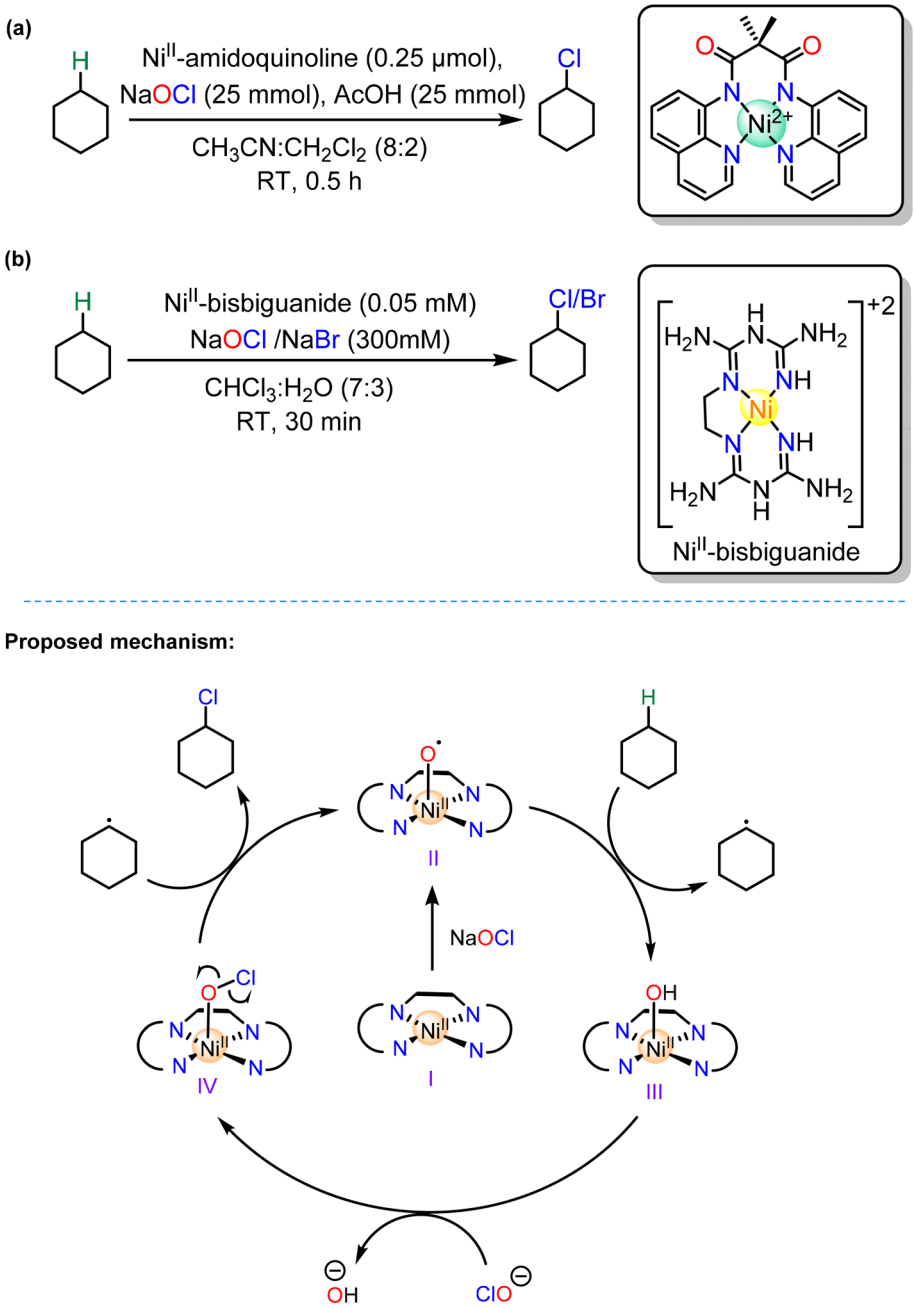

Fig. 12 (a) Ni(II)-(amidoquinoline) as a catalyst for the chlorination of alkanes. (b) Ni(II) complexes supported by the bisbiguanide ligand and its activity towards halogenation.

Open Access Article. Published on 14 November 2025. Downloaded on 3/15/2026 5:31:30 AM.
This article is licensed under a Creative Commons Attribution-NonCommercial 3.0 Unported Licence.

suggest that both pathways share a common rate-determining hydrogen atom transfer (HAT) step. The nature of the reaction environment, specifically, the presence of acid, plays a critical role in dictating the fate of the resulting carbon-centered radical, favouring halogenation over oxygenation under acidic conditions.

3.2 Porphyrin-based catalysts

In 2010, Groves and his co-workers demonstrated that a highly electron-deficient manganese porphyrin, Mn(TPFPP)Cl, efficiently and selectively catalyzes C–H chlorination and bromination of various simple alkanes in dichloromethane

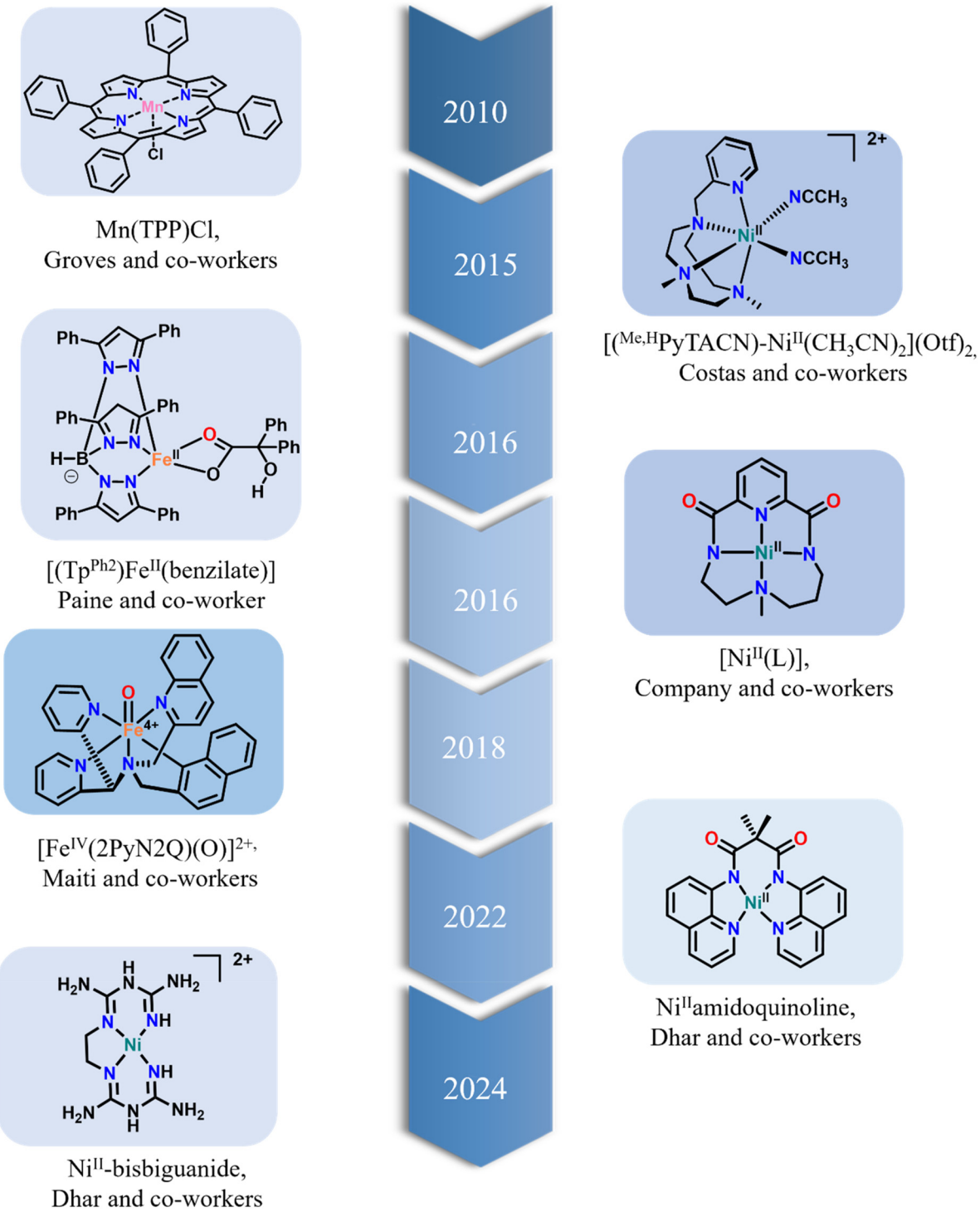

Fig. 13 First-row transition metal-based catalysts for C–H chlorination and bromination from 2010 onwards.

Open Access Article. Published on 14 November 2025. Downloaded on 3/15/2026 5:31:30 AM.
This article is licensed under a Creative Commons Attribution-NonCommercial 3.0 Unported Licence.

(DCM) at room temperature (RT) (Table 1 and Fig. 9).[43] Mechanistic studies showed that the reactive oxomanganese(v) species readily abstracts a hydrogen atom from a substrate C–H bond (supported by the kinetic isotope effect (KIE); a large magnitude of kinetic isotopic effect value of 8.7 ± 0.7 is observed for Mn(TPP)Cl, indicating that C–H abstraction is the rate-limiting step as the radicals like ClO• and Cl• show lower kinetic isotope effect values), forming a substrate-derived

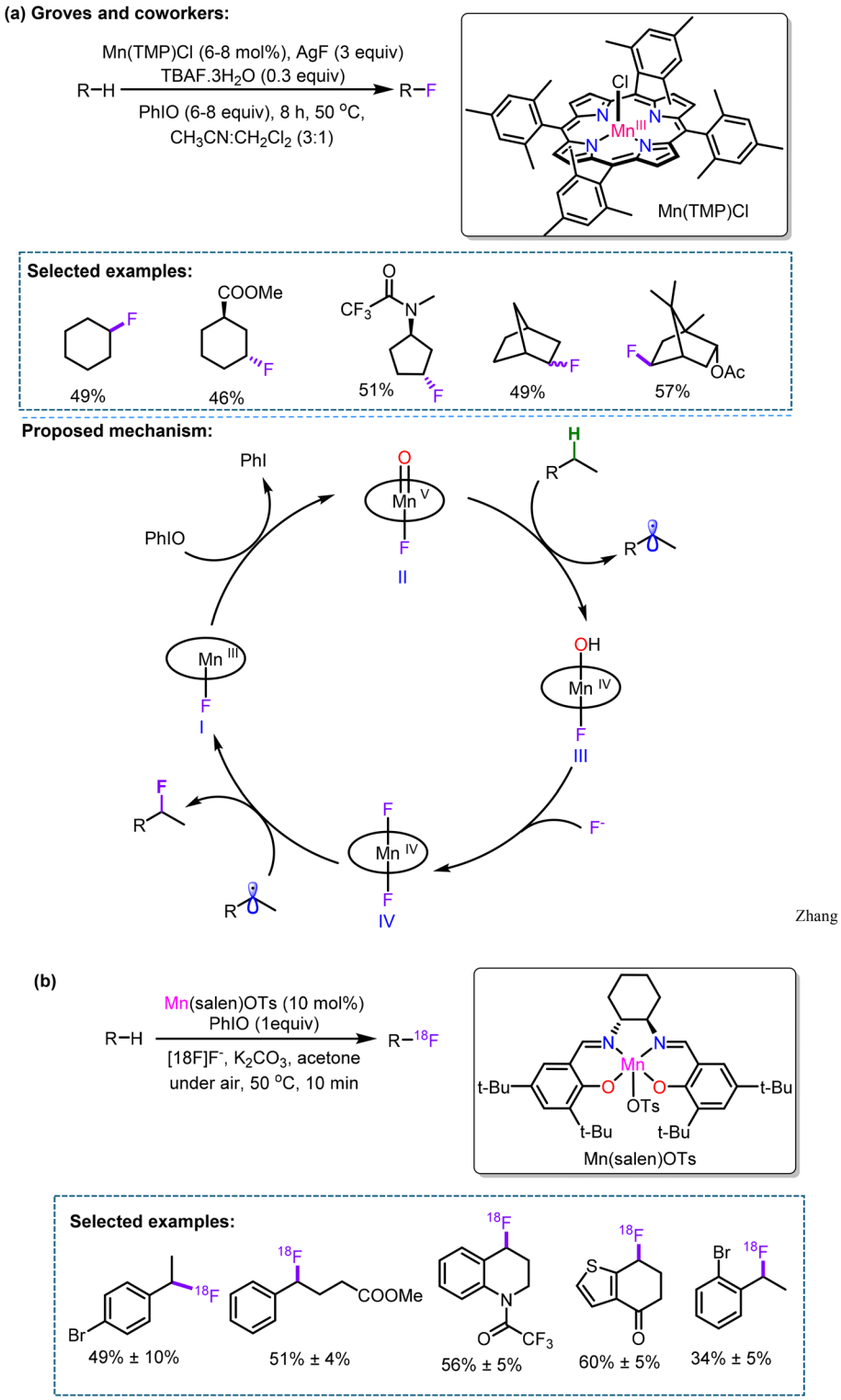

Fig. 14 Fluorination using (a) Mn(TMP)Cl catalyst, (b) Mn(Salen)Cl catalyst, both the catalysts facilitated the transfer of fluoride to a broad range of hydrocarbons when used alongside a hypervalent iodine-based oxidant and AgF and TBAF·3H_2O as fluoride sources.

Open Access Article. Published on 14 November 2025. Downloaded on 3/15/2026 5:31:30 AM.
This article is licensed under a Creative Commons Attribution-NonCommercial 3.0 Unported Licence.

radical and an HO-Mn^{IV}(por) intermediate. The HO-Mn^{IV} intermediate then exchanges the hydroxyl ligand with excess hypochlorite anions, transferring chlorine to the alkyl radical.

3.3. Nickel-based catalysts

The Costas group used a Ni(II) catalyst [(^{Me,H}PyTACN)-Ni^{II}(CH$_3$CN)$_2$](OTf)$_2$, with a robust triazacyclononane ligand (L = ^{Me,H}PyTACN) for the chlorination of alkanes with NaOCl as the terminal oxidant and chloride source (Table 1 and Fig. 10).[44] Reaction of NaOCl with [(^{Me,H}PyTACN)-Ni^{II}(CH$_3$CN)$_2$](OTf)$_2$ in acetonitrile generated a transient nickel(II)-hypochlorite species, [(L)NiII-OCl(S)]$^+$ (A), where S = solvent. The intermediate was identified by electrospray ionization mass spectrometry (ESI-MS). Spectroscopic studies such as UV-Vis absorption, electron paramagnetic resonance (EPR), and resonance Raman spectroscopy, *etc.*, indicate that intermediate **I** undergoes decay to yield the corresponding nickel(III)-hydroxo complex, [(L)Ni^{III}-OH(S)]$^{2+}$ (**II**), presumably *via* homolytic cleavage of the O–Cl bond with concomitant release of a Cl$^{\bullet}$ radical. Under the reaction conditions, hydrolysis of acetonitrile to acetic acid leads to the formation of the nickel(III)-acetate species, [(L)Ni^{III}-OOCCH$_3$(S)]$^{2+}$ (**III**), which is subsequently reduced to the nickel(II) analogue, [(L)Ni^{II}OOCCH$_3$(S)]$^{2+}$ (**IV**), likely *via* a reaction with OCl$^-$ or ClO$_2^-$. Upon reintroduction of NaOCl to complex **IV**, regeneration of **II** occurs more rapidly and in higher yield. According to the report, the addition of acids such as acetic acid or triflic acid significantly enhances both the rate and extent of formation of intermediate (**II**), suggesting that protonation facilitates O–Cl bond homolysis and promotes the generation of reactive high-valent nickel-oxo species. Later, the Company group used Ni(II) complexes with tetradentate macrocyclic bis(amidate) ligands (Table 1 and Fig. 11), showing promising reactivity toward alkanes at −30 °C in the presence of NaOCl.[45] DFT calculations suggested the formation of a nickel-hypochlorite species. Experimental and computational analyses indicate that the intermediate is best formulated as a Ni^{III} complex with one unpaired electron delocalized in the ligands surrounding the metal centre.

In 2022, our research group reported that Ni(II) complexes supported by an amido-quinoline ligand (Tables 1, 2 and Fig. 12a) effectively catalysed C–H chlorination of a series of hydrocarbons in the presence of NaOCl and acetic acid at RT in CH$_2$Cl$_2$/CH$_3$CN (2 : 8 v/v).[46a] Bond dissociation energy of the C(sp^3)–H bond of the substrates varies from 99.3 kcal mol^{-1} (cyclohexane) to 87 kcal mol^{-1} (ethyl benzene). Exclusively chlorinated products (TON: 220 for cyclohexane) were obtained without any hydroxylated products and thus mimicking the activity of the halogenase enzyme (Table 2 and Fig. 12).[46a] Inspired by our work, Thomas R. Ward's research group, biotinylated Ni(II)-(amido-quinoline) complexes within strepravidin.[46b] The resulting artificial nickel chlorinase was also efficient for the chlorination of diverse C(sp^3)–H bonds in an acetonitrile–phosphate buffer mixture. However, the solubility and stability of first-row transition metal catalysts in an aqueous medium are the major challenges. Therefore, synthetic chemists are trying to develop a new catalyst capable of achieving selective halogenation in an aqueous medium. Recently, Khatri *et al.* described that water-soluble guanidine complexes of Ni(II) (Fig. 12b) successfully chlorinate various hydrocarbons in the presence of NaOCl and acetic acid in a water and chloroform mixture (7 : 3) at RT (TON ~680 for cyclohexane) (Table 2).[47] The KIE (k_H/k_D) value was found to be

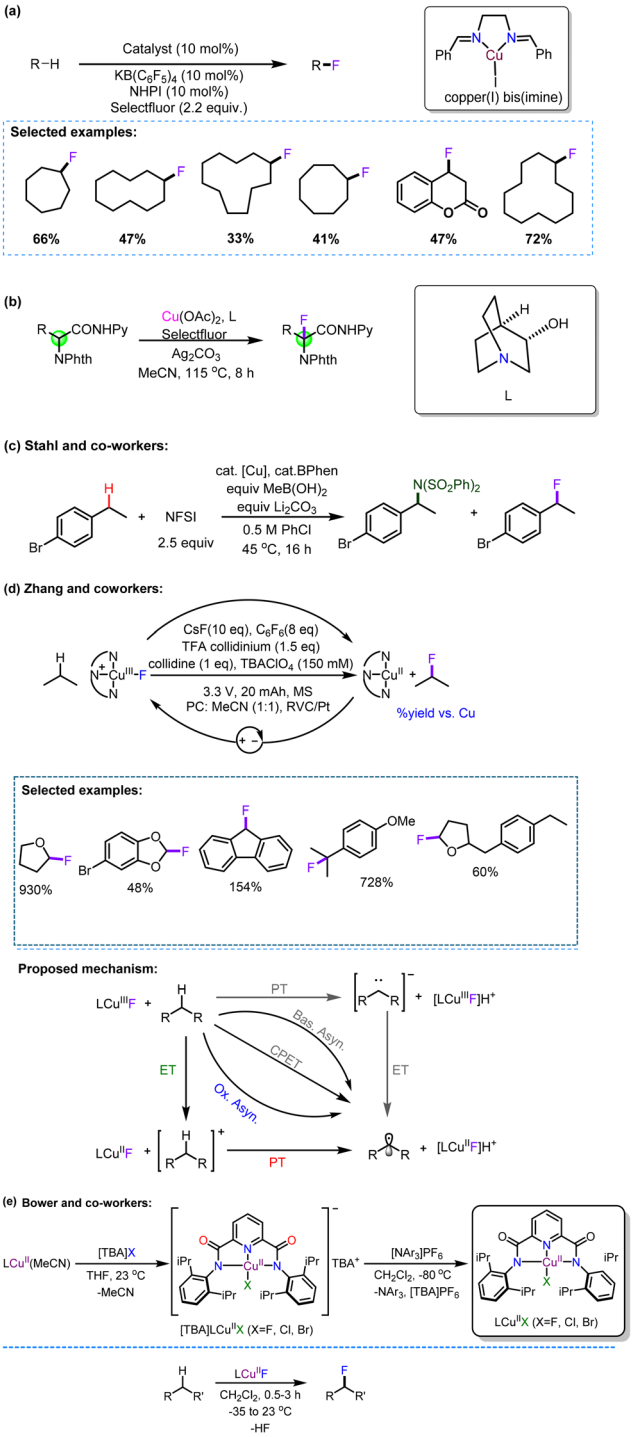

Fig. 15 (a–c) Cu-catalysed C(sp^3)–H fluorination; (d) organic electrochemical strategy for C(sp^3)–H fluorination; 1 TON = 100% yield *vs.* Cu. (e) C(sp^3)–H fluorination by a copper(III) fluoride complex.

Open Access Article. Published on 14 November 2025. Downloaded on 3/15/2026 5:31:30 AM.
This article is licensed under a Creative Commons Attribution-NonCommercial 3.0 Unported Licence.

12.2. It is suggested that C–H abstraction is the rate-determining step. Moreover, bromination was also carried out by *in situ* generation of NaOBr using an equimolar mixture of NaOCl and NaBr. A minimal amount of chlorinated product was found with the brominated product (Table 2).[47] Fig. 13 illustrates the progression of first-row transition metal-based catalytic systems reported since 2010 for the direct halogenation of C–H bonds, specifically targeting chlorination and bromination transformations.

4. Fluorination

C–H fluorination is exceedingly rare in nature, and living organisms have scarcely evolved a dedicated biochemistry for fluorine. A few tropical and subtropical plants are known to produce fluoroacetate, although its biosynthetic pathway remains poorly understood.[48] Moreover, reports of other naturally occurring fluorinated compounds are often viewed with caution, as they may result from contamination by anthropogenic or industrial sources rather than true biological synthesis. Nowadays, carbon–fluorine bonds are becoming increasingly crucial components in pharmaceuticals, agrochemicals, and positron emission tomography (PET) tracers.[49] Among the top 200 pharmaceutical products by retail sales in 2016, 36 contain fluorine.[50] In recent years, numerous methods have been developed for incorporating fluorine into small molecules. However, relatively few studies focus on direct fluorination.[51] This approach is particularly appealing due to its efficiency and potential for late-stage functionalization, enabling rapid access to complex, fluorinated analogues of high value. Despite these advantages, the inherent

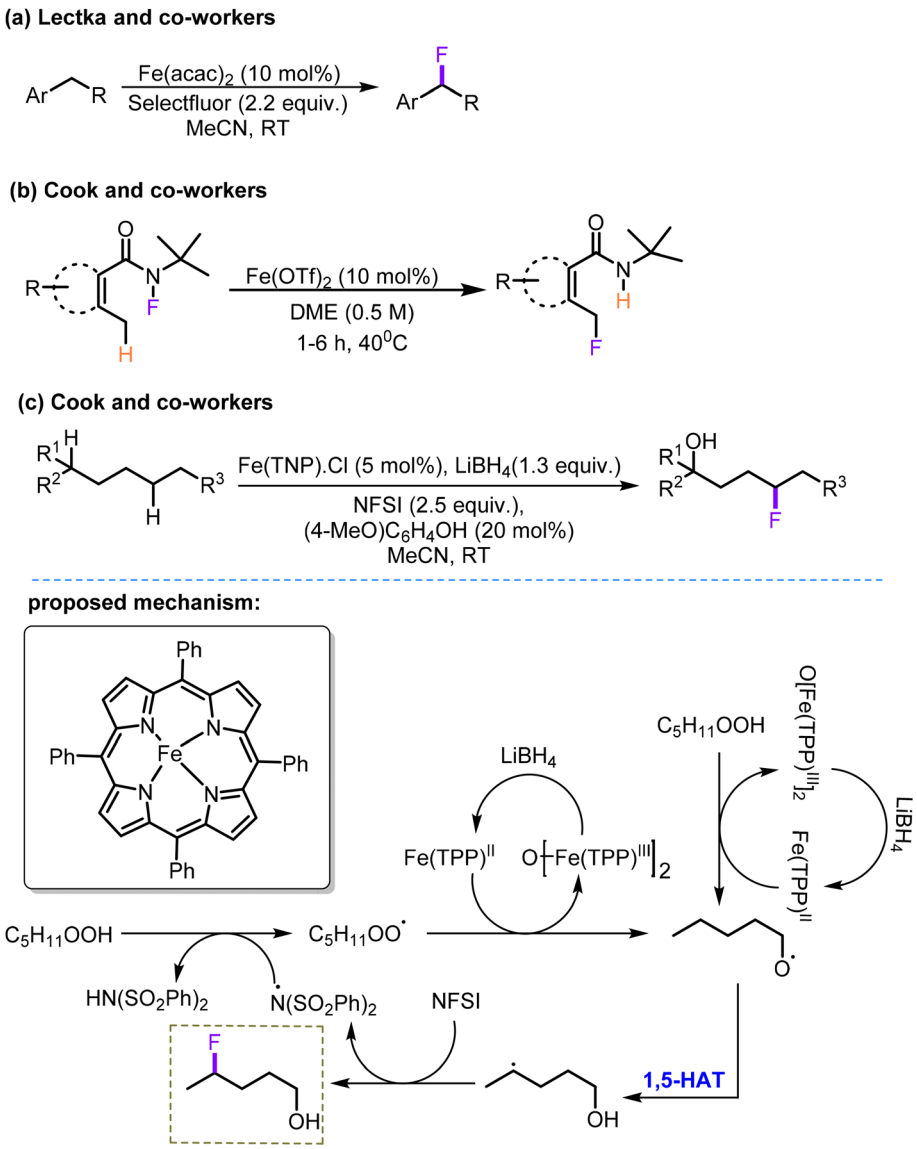

Fig. 16 (a–c) Iron-catalysed C(sp^3)–H fluorination.

Open Access Article. Published on 14 November 2025. Downloaded on 3/15/2026 5:31:30 AM.
This article is licensed under a Creative Commons Attribution-NonCommercial 3.0 Unported Licence.

challenges of C–H fluorination have limited the number of successful examples, especially when compared to other halogenation strategies. In the context of C–F bond formation, several additional obstacles complicate direct fluorination. Notably, the strong metal–fluorine interactions and the high hydration energy of fluoride ions often result in substantial reaction barriers. Although C–F bonds are thermodynamically stable, with bond dissociation energies exceeding 100 kcal mol^{-1},[52] the use of fluoride salts as fluorine sources can be problematic due to their high lattice energies, which limit their reactivity. Electrophilic fluorinating reagents present a more reactive alternative, circumventing some of these issues, but they are typically more costly and less atom-economical than fluoride-based reagents. Considering both the intrinsic difficulties of C–H functionalization and the unique challenges associated with C–F bond formation, it is perhaps unsurprising that direct C–H fluorination remains a relatively underdeveloped area in synthetic chemistry.

C–H fluorination could be classified as directed C–H fluorination, aromatic C–H fluorination, and aliphatic C–H fluorination. Directed C–H fluorination and aromatic C–H fluorination are mostly carried out using second- and third-row transition metal catalysts. In this review, we are focusing on the application of first-row transition metal-based catalysts in C(sp^3)–H fluorination. These synthetic methods require extreme and non-biological conditions to overcome the high C–H bond dissociation energy and the low nucleophilicity of the fluoride ion.

4.1 Aliphatic C–H fluorination

Groves and co-workers demonstrated that various manganese catalysts, such as Mn(TMP)Cl, Mn(Salen)Cl, and Mn(TPFPP)Cl, can facilitate the transfer of fluoride to a broad range of hydrocarbons when used alongside a hypervalent iodine-based oxidant and AgF and TBAF·$3H_2O$ as fluoride sources (Fig. 14a).[53] Mechanistic studies indicate that the regioselectivity of C–H bond activation is governed by an oxomanganese(v) catalytic intermediate. However, the competing hydroxide rebound reaction is a key challenge in these processes. Later, the Groves group further achieved the Mn(salen)OT-catalyzed ^{18}F-radiofluorination of benzylic C(sp^3)–H bonds with a no-carrier added [^{18}F]-fluoride ion (Fig. 14b).[54] This approach employs Mn(salen)OTs as the fluoride transfer catalyst, enabling efficient labelling of various bioactive molecules and building blocks with radiochemical yields between 20% and 72% within 10 minutes.

Lectka and collaborators reported that combining Selectfluor (SF) and CuI in the presence of diamine ligands enables C(sp^3)–H bond fluorination, yielding fluorinated products in modest to good yields (up to 75%) (Fig. 15a).[55] It was found that the addition of *N*-hydroxyphthalimide and potassium iodide could improve the yield of this reaction and facili-

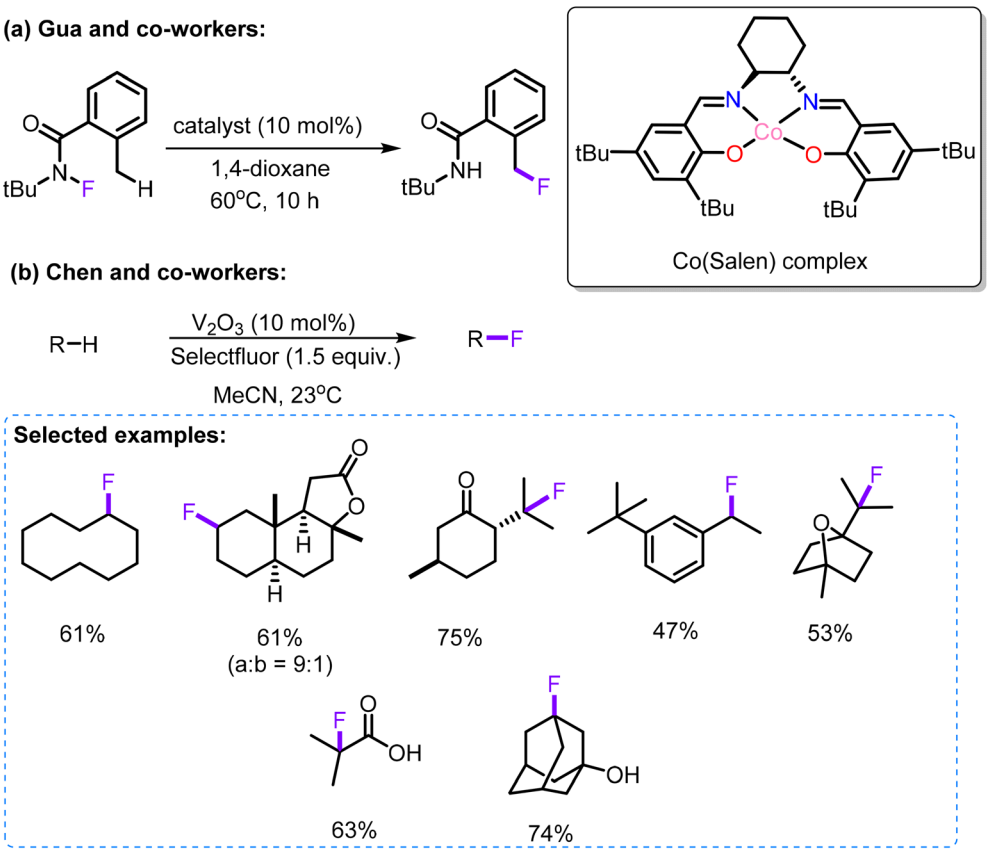

Fig. 17 C(sp^3)–H fluorination using (a) Cobalt-catalyst (b) Vanadium-catalyst.

Open Access Article. Published on 14 November 2025. Downloaded on 3/15/2026 5:31:30 AM.
This article is licensed under a Creative Commons Attribution-NonCommercial 3.0 Unported Licence.

tate the regeneration of the Cu(I) catalyst as well. In 2018, Liu and co-workers reported a novel Cu(II)-catalyzed α-C(sp^3)–H fluorination of amino acid derivatives using Selectfluor as the fluorine source (Fig. 15b).[56] Notably, the addition of (*R*)-3-hydroxyquinuclidine was found to significantly enhance the reaction yield. The proposed mechanism involves initial pre-coordination of $Cu(OAc)_2$ with (*R*)-3-hydroxyquinuclidine, which is believed to facilitate the catalytic process. In 2020, Stahl and co-workers reported a Cu(I)-catalyzed benzylic C(sp^3)–H fluorination reaction using *N*-fluorobenzenesulfonimide (NFSI) as the fluorinating agent (Fig. 15c).[57] In 2023, the Zhang group developed an organic electrochemical strategy for C(sp^3)–H fluorination, enabling the synthesis of a broad range of alkyl fluorides *via* a Cu(BCAP)(MeCN)-catalyzed process (Fig. 15d).[58] This work built upon their earlier studies involving a stoichiometric copper(III) reagent, now advancing to a catalytic system. To prevent the undesired reduction of Cu(II) at the cathode, hexafluorobenzene (C_6F_6) was employed as a sacrificial electron acceptor. Substrate scope investigations revealed a clear preference for fluorination at C–H bonds adjacent to oxygen atoms over benzylic C–H sites, highlighting the method's selectivity and synthetic utility. In 2025, Díaz *et al.* reported a copper(I)-initiated, site-selective β–ζ-C(sp^3)–H bond fluorination of ketones, carboxylic esters, and amides using Selectfluor as the fluorine source.[59] This methodology demonstrates high site selectivity in C(sp^3)–F bond formation and was successfully applied to the late-stage functionalization of complex natural products and pharmaceutical derivatives, highlighting its potential utility in medicinal chemistry and molecular diversification.

In 2020, Bower and colleagues reported the C(sp^3)–H fluorination by a copper(III) fluoride complex (Fig. 15e).[58b] Mechanistic studies using a triphenylmethyl radical probe revealed that the complex, LCuF, engages in radical capture through a concerted pathway. Notably, LCuF demonstrated the ability to mediate both hydrogen atom abstraction and radical capture, enabling efficient fluorination of allylic and benzylic C–H bonds, as well as α-C–H bonds of ethers, under mild, room-temperature conditions.

In 2013, the Lectka group reported an Fe(II)-catalyzed C(sp^3)–H fluorination of alkylbenzenes using Selectfluor as the fluorine source (Fig. 16a).[60] The reaction goes through a radical pathway. The Cook group reported a mild, iron-mediated, amide-directed C–H fluorination of benzylic, allylic, and unactivated positions (Fig. 16b).[61] In this method, *N*-fluoro-2-methylbenzamides undergo chemoselective fluorine transfer upon treatment with a catalytic amount of iron(II) triflate ($Fe(OTf)_2$), affording the corresponding fluorinated products in high yields. The reaction exhibits broad substrate scope and excellent functional group tolerance, all without the need for noble metal catalysts. Mechanistic and computational studies support a pathway involving short-lived radical intermediates, with fluorine transfer occurring directly through an iron-mediated process. An alkoxyl radical-guided strategy for site-selective functionalization of unactivated methylene and methine C–H bonds, enabled by an Fe^{II}-catalyzed redox process, is described by the Liu group (Fig. 16c).[62]

Guo and team developed a redox-neutral, radical-relay cobalt-catalyzed intramolecular C–H fluorination of

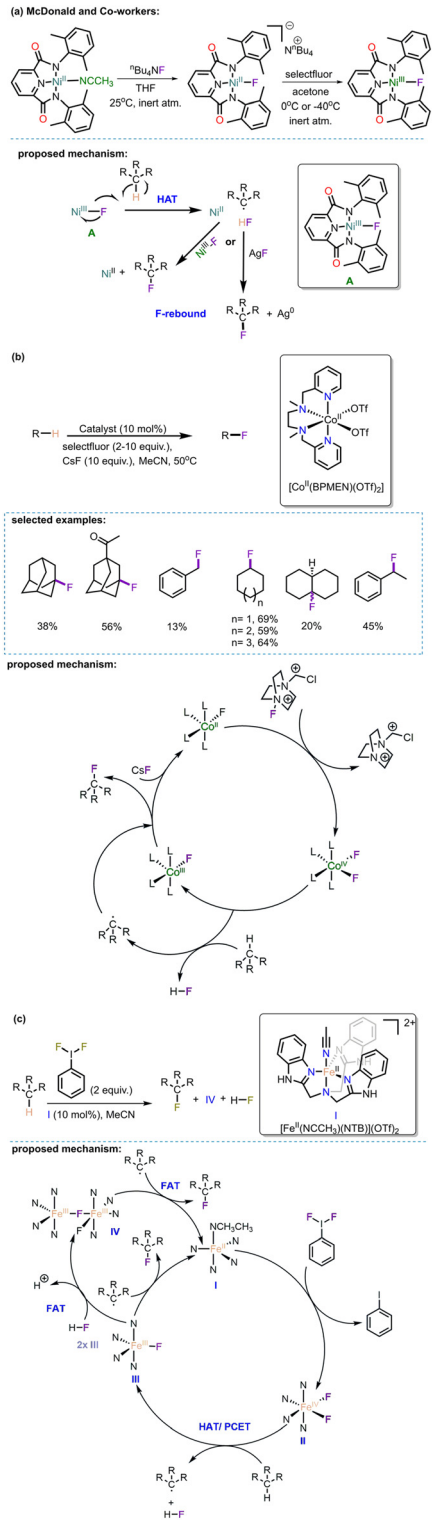

Fig. 18 (a) Nickel-catalysed, (b) Cobalt-catalysed and (c) Iron-catalysed C(sp^3)–H fluorination developed by McDonald and his research group.

Open Access Article. Published on 14 November 2025. Downloaded on 3/15/2026 5:31:30 AM.
This article is licensed under a Creative Commons Attribution-NonCommercial 3.0 Unported Licence.

N-fluoroamides, in which cobalt fluorides, formed *in situ*, act as latent radical fluorinating agents (Fig. 17a).[63] The Chen group reported direct fluorination to the tertiary position of 1,4-cineole and L-menthone selectively with Selectfluor using vanadium(III) oxide as a catalyst (Fig. 17b).[64]

McDonald and co-workers showed that high-valent first-row transition metal–fluoride complexes, such as the Ni–F complex $[Ni^{III}(F)(L)]$ (L = *N*,*N*′-(2,6-dimethylphenyl)-2,6-pyridinedicarboxamidate), can oxidize hydrocarbons *via* a hydrogen atom transfer (HAT) mechanism while also promoting oxidative fluorination (Fig. 18a).[65] The same group further reported that the complex $[Fe^{II}(NCCH_3)(NTB)](OTf)_2$ (NTB = tris(2-benzimidazoylmethyl)amine; OTf = trifluoromethanesulfonate) reacts with difluoro(phenyl)-λ^3-iodane ($PhIF_2$) in the presence of saturated hydrocarbons to produce fluorinated products in moderate to good yields *via* a dimeric μ-F-$(Fe^{III})_2$ intermediate (Fig. 18b).[66] They also found that polyamine-supported Co(II) complexes in the presence of SF and CsF catalyze the oxidative fluorination of saturated hydrocarbons (Fig. 18c).[67] These reactions can deliver near-quantitative yields, and a mechanistic study reveals the involvement of a Co(IV)–$(F)_2$ species in C–H activation, followed by fluorine atom transfer from a Co(III)–F intermediate during radical rebound.

5. Asymmetric C–H halogenation

Optically active halocarbon compounds play a crucial role in areas such as organic synthesis, natural product chemistry, and biomedical and pharmaceutical sciences; however, catalytic enantioselective formation of halogenated chiral carbon centres through C–X bond-forming reactions remains exceptionally rare. In 2000, Togni and co-workers were the first to report a catalytic, enantioselective fluorination of β-ketoesters (activated $C(sp^3)$–H bond) using Selectfluor as the fluorine source and chiral $[TiCl_2(TADDOLato)]$ complexes as the catalyst in acetonitrile at RT (Fig. 19). For a substituted benzyl ester substrate, they achieved an enantiomeric excess (ee) of 90%.[68] The same $[TiCl_2(TADDOLato)]$ complexes catalyzed the one-pot enantioselective heterodihalogenation of β-ketoesters with Selectfluor and *N*-chlorosuccinimide (NCS) to afford α-chloro-α-fluoro-β-ketoesters in moderate to good yields (up to 65% ee).[69]

Lectka and co-workers have developed a catalytic and highly enantioselective method (up to >99% ee) for the α-fluorination of acid chlorides, enabling the synthesis of a broad range of optically active carboxylic acid derivatives from readily available and commercially accessible starting materials (Fig. 20).[70] The transformation proceeds *via* dually activated ketene enolate intermediates, which are generated through the cooperative action of two discrete catalysts: a chiral nucleophile and an achiral Ni(II) complex operating in tandem. The resulting α-fluorobis(sulfonimide) intermediates are highly reactive and undergo efficient *in situ* transacylation under mild conditions upon the addition of diverse nucleophiles, including structurally complex natural products.

Marigo *et al.* reported the first catalytic enantioselective halogenation, specifically chlorination and bromination of both acyclic and cyclic β-ketoesters, as well as a β-diketone. Using NCS and *N*-bromosuccinimide (NBS) as halogen sources in combination with chiral bisoxazoline copper(II) complexes,

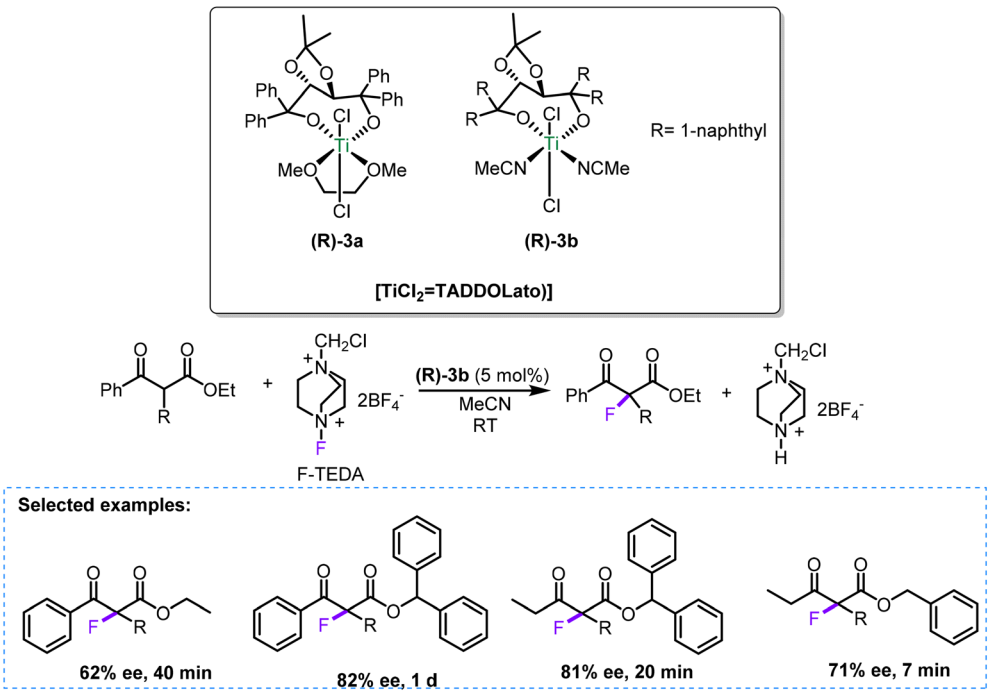

Fig. 19 Togni's catalyst for enantioselective fluorination of β-ketoesters.

Open Access Article. Published on 14 November 2025. Downloaded on 3/15/2026 5:31:30 AM.
This article is licensed under a Creative Commons Attribution-NonCommercial 3.0 Unported Licence.

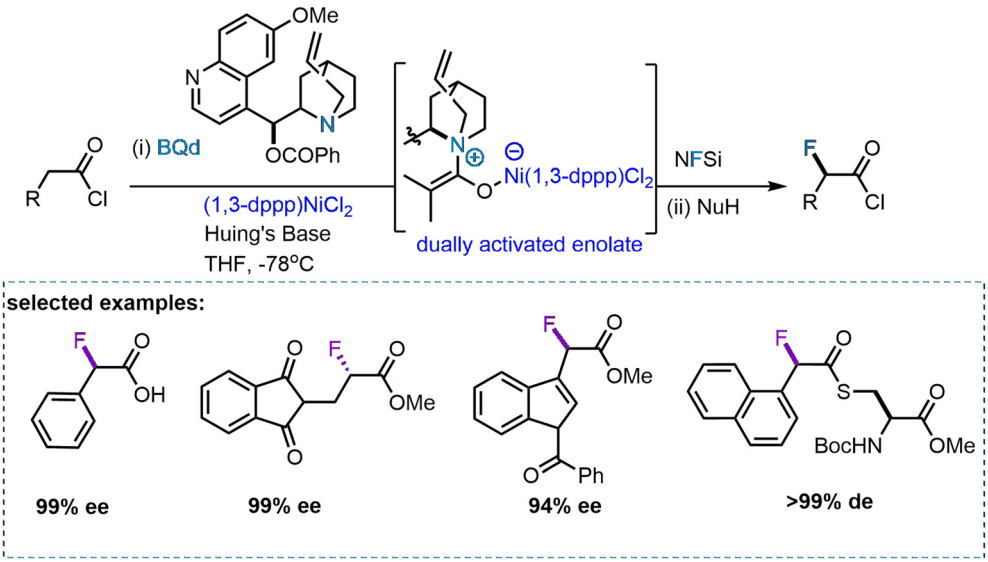

Fig. 20 α-Fluorination of acid chlorides *via* cooperative action of two discrete catalysts: a chiral nucleophile and an achiral Ni(II) complex.

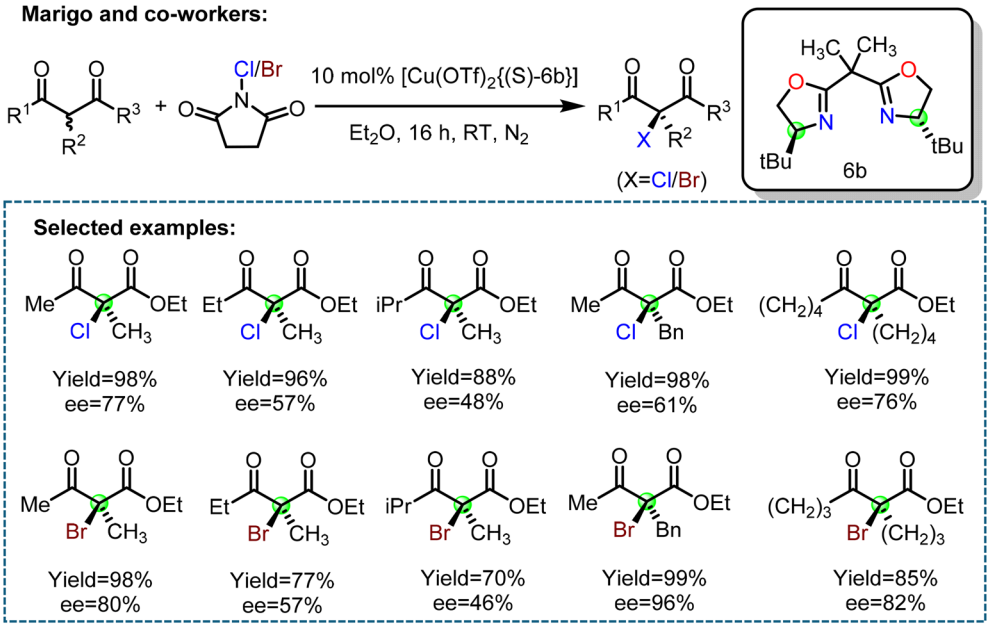

Fig. 21 Enantioselective halogenation of both acyclic and cyclic β-ketoesters, and β-diketone using NCS and NBS as halogen sources in combination with chiral bisoxazoline copper(II) complexes.

they obtained the corresponding optically active α-halogenated products in excellent yields and with moderate to good enantioselectivities (Fig. 21).[71] Frings *et al.* developed an asymmetric halogenation of cyclic and acyclic β-oxoesters using a sulfoximine–copper complex, producing α-bromo-, α-chloro-, and α-fluoro-compounds in high yields and with moderate to good enantioselectivity.[72] Shibatomi *et al.* further advanced enantioselective halogenation by employing a chiral Lewis acid catalyst formed from $Cu(OTf)_2$ and a newly designed spirooxazoline ligand. This system enabled the α-chlorination of β-ketoesters and malonates with excellent enantioselectivity, reaching up to 98% ee.[73] Reddy *et al.* achieved highly enantioselective fluorination of aryl acetyl- and 3-butenoyl-substituted thiazolidinones using a combinatorial catalytic system composed of DBFOX-Ph/Ni(II)/HFIP/2,6-lutidine, providing an efficient route to chiral α-fluorinated compounds.[74]

Open Access Article. Published on 14 November 2025. Downloaded on 3/15/2026 5:31:30 AM.
This article is licensed under a Creative Commons Attribution-NonCommercial 3.0 Unported Licence.

6. Conclusions

Halogenating enzymes have the potential to play a significant role in future "white" biotechnology. However, several aspects must be optimized before these enzymes gain widespread use in industrial biocatalysis. In contrast, transition metal-catalyzed C–H activation has opened new avenues for synthesizing a broader range of halogenated compounds by enabling more selective halogenation of difficult substrates. As summarized in this review, significant progress has been achieved in the C(sp^3)–H halogenation field through the use of manganese, iron, cobalt, nickel, and copper catalysts, greatly expanding the synthetic toolbox for accessing halogenated compounds. However, to date, a major challenge in C(sp^3)–H functionalization lies in achieving precise site selectivity amid the multitude of similar C–H bonds within a molecule.[75] Future research is expected to address this issue through the development of innovative strategies aimed at enhancing selectivity and control. The design of catalysts and ligands will play a pivotal role in overcoming the inherent reactivity differences among primary, secondary, and tertiary C–H bonds, enabling selective and remote C–H functionalization. Integrating computational modeling to predict and guide the development of highly selective catalyst–ligand systems is expected to accelerate advances in this area.

The development of general and high-yielding methods for asymmetric C(sp^3)–H halogenation remains a significant challenge. Success in this area would represent a breakthrough, offering powerful new tools for the synthesis of chiral pharmaceuticals and fine chemicals. Recent advances have demonstrated that earth-abundant metals such as nickel and cobalt can enable enantioconvergent radical transformations.[75] This emerging strategy holds significant promise for the synthesis of chiral molecules and is poised for further expansion.

Furthermore, to facilitate the translation of these diverse methodologies from academic research to industrial practice, the implementation of flow technology could be a promising approach. Flow systems offer superior heat and mass transfer, enhanced safety over conventional batch processes, and are especially well-suited for managing highly reactive intermediates. Furthermore, the intrinsic scalability of flow chemistry makes it an attractive platform for large-scale applications.

Conflicts of interest

There are no conflicts to declare.

Data availability

This review article does not include the generation or analysis of original data; therefore, a data availability statement is not applicable.

Acknowledgements

BBD acknowledges CSIR, New Delhi (grant no. EMR-II 80 (0086)/17), and SERB, DST (CRG/2022/001576), for funding. Monika, JK, KD, RC and SKY acknowledge SNIoE and Shiv Nadar Foundation for a fellowship. Monika acknowledges CSIR, New Delhi, for an SRF fellowship.

References

1 (*a*) P. Jeschke, *Pest Manage. Sci.*, 2017, **73**, 1053–1066; (*b*) An HIS Economic Report: The benefits of chlorine chemistry in pharmaceuticals in the United States and Canada, R. Whitfield and F. Brown, 2016 (*c*) D. Cantillo and C. O. Kappe, *React. Chem. Eng.*, 2017, **2**, 7–19; (*d*) P. Jeschke, *Pest Manage. Sci.*, 2024, **80**, 3065–3087.
2 P. Jeschke, R. Nauen, M. Schindler and A. Elbert, *J. Agric. Food Chem.*, 2011, **59**, 2897–2908.
3 G. W. Gribble, *Environ. Chem.*, 2015, **12**, 396–405.
4 F. J. Alvarez-Martinez, E. Barrajon-Catalan and V. Micol, *Biomedicines*, 2020, **8**, 405.
5 (*a*) A Proclamation on the 50th Anniversary of the National Cancer Act of 1971. Available online: https://www.whitehouse.gov/briefing-room/presidential-actions/2021/12/22/a-proclamation-on-the-50th-anniversary-of-the-national-cancer-act-of-1971/ (accessed on 5 February 2022); (*b*) R. M. Lunn, S. S. Mehta, G. D. Jahnke, A. Wang, M. S. Wolfe and B. R. Berridge, *J. Natl. Cancer Inst.*, 2022, **114**, 1441–1448.
6 G. Chandra, D. V. Singh, G. K. Mahato and S. Patel, *Chem. Pap.*, 2023, **77**, 4085–4106.
7 G. M. Keating, *Drugs*, 2015, **75**, 675–685.
8 D. B. Tiz, L. Bagnoli, O. Rosati, F. Marini, L. Sancineto and C. Santi, *Molecules*, 2022, **27**, 1643.
9 S. Moreno, C. F. Perno, P. W. Mallon, G. Behrens, P. Corbeau, J. P. Routy and G. Darcis, *HIV Med.*, 2019, **20**, 2–12.
10 J. M. Molina and S. L. Cox, *Drugs Today*, 2005, **41**, 241–252.
11 M. M. Bastos, C. C. P. Costa, T. C. Bezerra, F. C. Silva and N. Boechat, *Eur. J. Med. Chem.*, 2016, **108**, 455–465.
12 C. Crowe, S. Molyneux, S. V. Sharma, Y. Zhang, D. S. Gkotsi, H. Connaris and R. J. M. Goss, *Chem. Soc. Rev.*, 2021, **50**, 9443–9481.
13 F. H. Vaillancourt, J. Yin and C. T. Walsh, *Proc. Natl. Acad. Sci. U. S. A.*, 2005, **102**, 10111–10116.
14 G. T. Hofler, A. But and F. Hollmann, *Org. Biomol. Chem.*, 2019, **17**, 9267–9274.
15 (*a*) C. Dong, S. Flecks, S. Unversucht, C. Haupt, K. H. V. Pee and J. H. Naismith, *Science*, 2005, **309**, 2216–2219; (*b*) B. F. Fischer, H. M. Snodgrass, K. A. Jones, M. C. Andorfer and J. C. Lewis, *ACS Cent. Sci.*, 2019, **5**, 1844–1856.
16 Z. F. Blazevic, N. Milcic, M. Sudar and M. M. Elenkov, *Adv. Synth. Catal.*, 2021, **363**, 388.
17 K. Faber and W. Kroutil, *Curr. Opin. Chem. Biol.*, 2005, **9**, 181–187.

 This journal is © The Royal Society of Chemistry 2026

Open Access Article. Published on 14 November 2025. Downloaded on 3/15/2026 5:31:30 AM.
This article is licensed under a Creative Commons Attribution-NonCommercial 3.0 Unported Licence.

18 N. Kasai, T. Suzuki and Y. Furukawa, *J. Mol. Catal. B: Enzym.*, 1998, **4**, 237–252.
19 S. K. Ma, J. Gruber, C. Davis, L. Newman, D. Gray, A. Wang, J. Grate, G. W. Huisman and R. A. Sheldon, *Green Chem.*, 2010, **12**, 81–86.
20 S. Pandian, M. A. Vincent, I. H. Hillier and N. A. Burton, *Dalton Trans.*, 2009, 6201–6207.
21 R. H. Wilson, S. Chatterjee, E. R. Smithwick, A. R. Damodaran and A. B. Damodaran, *ACS Catal.*, 2024, **14**, 13209–13218.
22 (*a*) F. H. Vaillancourt, J. Yin and C. Walsh, *Proc. Natl. Acad. Sci. U. S. A.*, 2005, **102**, 10111–10116; (*b*) J. C. Price, E. W. Barr, B. Tirupati, J. M. Bollinger and C. Krebs, *Biochemistry*, 2003, **42**, 7497–7508.
23 G. T. Hofler, A. But and F. Hollmann, *Org. Biomol. Chem.*, 2019, **17**, 9267–9274.
24 (*a*) B. A. Kaup, U. Piantini, M. Wüst and J. Schrader, *Appl. Microbiol. Biotechnol.*, 2007, **73**, 1087–1096; (*b*) U. Piantini, J. Schrader, A. Wawrzun and M. Wust, *Food Chem.*, 2011, **129**, 1025–1029; (*c*) B. A. Kaup, U. Piantini, M. Wust and J. Schrader, *Appl. Microbiol. Biotechnol.*, 2007, **73**, 1087–1096; (*d*) U. Piantini, J. Schrader, A. Wawrzun and M. Wust, *Food Chem.*, 2011, **129**, 1025–1029.
25 B. O. Burek, S. Bormann, F. Hollmann, J. Z. Bloh and D. Holtmann, *Green Chem.*, 2019, **21**, 3232–3249.
26 (*a*) N. Itoh, A. K. M. Q. Hasan, Y. Izumi and H. Yamada, *Eur. J. Biochem.*, 1988, **172**, 477–484; (*b*) H. Yamada, N. Itoh and Y. Izumi, *J. Biol. Chem.*, 1985, **260**, 1962–1969.
27 L. Getrey, T. Krieg, F. Hollmann, J. Schrader and D. Holtmann, *Green Chem.*, 2014, **16**, 1104–1108.
28 D. Wischang, M. Radlow and J. Hartung, *Dalton Trans.*, 2013, **42**, 11926–11940.
29 E. Fernández-Fueyo, M. van Wingerden, R. Renirie, R. Wever, Y. Ni, D. Holtmann and F. Hollmann, *ChemCatChem*, 2015, **7**, 4035–4038.
30 (*a*) C. Dong, S. Flecks, S. Unversucht, C. Haupt, K.-H. V. Pee and J. H. Naismith, *Science*, 2005, **309**, 2216–2219; (*b*) B. F. Fisher, H. M. Snodgrass, K. A. Jones, M. C. Andorfer and J. C. Lewis, *ACS Cent. Sci.*, 2019, **5**, 1844–1856.
31 (*a*) A. Lang, S. Polnick, T. Nicke, P. William, E. P. Patallo, J. H. Naismith and K. H. Van Pèe, *Angew. Chem., Int. Ed.*, 2011, **50**, 2951–2953; (*b*) S. Zehner, A. Kotzsch, B. Bister, R. D. Süssmuth, C. Méndez, J. A. Salas and K. H. van Pée, *Chem. Biol.*, 2005, **12**, 445–452; (*c*) T. Kittilä, C. Kittel, J. Tailhades, D. Butz, M. Schoppet, A. Büttner, R. J. A. Goode, R. B. Schittenhelm, K.-H. van Pee, R. D. Süssmuth, W. Wohlleben, M. J. Cryle and E. Stegmann, *Chem. Sci.*, 2017, **8**, 5992–6004; (*d*) D. R. M. Smith, A. R. Uria, E. J. N. Helfrich, D. Milbredt and K.-H. V. Pee, *ACS Chem. Biol.*, 2017, **12**, 1281–1287; (*e*) M. Ismail, L. Schroeder, M. Frese, T. Kottke, F. Hollmann, C. E. Paul and N. Sewald, *ACS Catal.*, 2019, **9**, 1389–1395.
32 D. H. R. Barton, *Chem. Soc. Rev.*, 1996, **25**, 237–239.
33 (*a*) D. H. R. Barton, E. Csuhai and D. Doller, *Tetrahedron*, 1992, **48**, 9195–9206; (*b*) D. H. R. Barton and D. Doller, *Acc. Chem. Res.*, 1992, **25**(11), 504–512.
34 (*a*) T. Kojima, R. A. Leising, S. Yan and L. Que Jr, *J. Am. Chem. Soc.*, 1993, **115**, 11328–11335; (*b*) I. W. C. E. Arends, K. U. Ingold and D. D. M. Wayner, *J. Am. Chem. Soc.*, 1995, **117**(16), 4710–4711.
35 H. Noack and P. E. M. Siegbahn, *J. Biol. Inorg. Chem.*, 2007, **12**, 1151–1162.
36 P. Comba and S. Wunderlich, *Chem. – Eur. J.*, 2010, **16**, 7293–7299.
37 O. Planas, M. Clémancey, J. M. Latour, A. Company and M. Costas, *Chem. Commun.*, 2014, **50**, 10887–10890.
38 M. Puri, A. N. Biswas, R. Fan, Y. Guo and L. Que Jr, *J. Am. Chem. Soc.*, 2016, **138**, 2484–2487.
39 (*a*) S. Chatterjee and T. K. Paine, *Angew. Chem., Int. Ed.*, 2016, **55**, 7717–7722; (*b*) R. D. Jana, D. Sheet, S. Chatterjee and T. K. Paine, *Inorg. Chem.*, 2018, **57**, 8769–8777.
40 (*a*) S. Rana, S. Bag, T. Patra and D. Maiti, *Adv. Synth. Catal.*, 2014, **356**, 2453–2458; (*b*) S. Rana, J. P. Biswas, A. Sen, M. Clémancey, G. Blondin, J. M. Latour, G. Rajaraman and D. Maiti, *Chem. Sci.*, 2018, **9**, 7843–7858; (*c*) S. Sasmal, S. Rana, G. K. Lahiri and D. Maiti, *J. Chem. Sci.*, 2018, **130**, 88.
41 J. Han, L. Tan, Y. Wan, G. Li and S. N. Anderson, *Dalton Trans.*, 2022, **51**, 11620–11624.
42 N. P. Vila, I. Gamba, M. Clémancey, J. M. Latour, A. Company and M. Costas, *J. Inorg. Biochem.*, 2024, **259**, 112643.
43 (*a*) W. Liu and J. T. Groves, *Acc. Chem. Res.*, 2015, **48**, 1727–1735; (*b*) W. Liu and J. T. Groves, *J. Am. Chem. Soc.*, 2010, **132**, 12847–12849; (*c*) X. Huang, T. M. Burgsten and J. T. Groves, *J. Am. Chem. Soc.*, 2015, **137**, 5300–5303.
44 A. Draksharapu, Z. Codolà, L. Gómez, J. Lloret-Fillol, W. R. Browne and M. Costas, *Inorg. Chem.*, 2015, **54**, 10656–10666.
45 T. Corona, A. Draksharapu, S. K. Padamati, I. Gamba, V. Martin-Diaconescu, F. Acuna-Parés, W. R. Browne and A. Company, *J. Am. Chem. Soc.*, 2016, **138**, 12987–12996.
46 (*a*) S. Adhikari, A. Sarkar and B. B. Dhar, *Chem. Commun.*, 2022, **58**, 4075–4078; (*b*) K. Yu, K. Zhang, R. P. Jakob, T. Maier and T. R. Ward, *Chem. Commun.*, 2024, **60**, 1944–1947.
47 J. Khatri, V. Mari, A. Sarkar, N. Karmodak and B. B. Dhar, *Dalton Trans.*, 2025, **54**, 503–510.
48 K. K. J. Chan and D. O. Hagan, *Methods Enzymol.*, 2012, **516**, 219–235.
49 (*a*) K. Muller, C. Faeh and F. Diederich, *Science*, 2007, **317**, 1881–1886; (*b*) S. Purser, P. R. Moore, S. Swallow and V. Gouverneur, *Chem. Soc. Rev.*, 2008, **37**, 320–330; (*c*) W. K. Hagmann, *J. Med. Chem.*, 2008, **51**, 4359–4369; (*d*) V. Gouverneur and K. Müller, *Fluorine in Pharmaceutical and Medicinal Chemistry*, World Scientific, England, 2012; (*e*) Y. Zhou, J. Wang, Z. Gu, S. Wang, W. Zhu, J. L. Acena, V. A. Soloshonok, K. Izawa and H. Liu, *Chem. Rev.*, 2016, **116**, 422–518.
50 N. A. McGrath, M. Brichacek and J. T. Njardarson, *J. Chem. Educ.*, 2010, **87**, 1348–1349.
51 T. Liang, C. N. Neumann and T. Ritter, *Angew. Chem., Int. Ed.*, 2013, **52**, 8214–8264.

Open Access Article. Published on 14 November 2025. Downloaded on 3/15/2026 5:31:30 AM.
This article is licensed under a Creative Commons Attribution-NonCommercial 3.0 Unported Licence.

52 J. A. Dean, in *Lange's Handbook of Chemistry*, McGraw-Hill, New York, St Louis, San Francisco, 1999.
53 (*a*) W. Liu and J. T. Groves, *Angew. Chem., Int. Ed.*, 2013, **52**, 6024–6027; (*b*) G. Li, A. K. Dilger, P. T. Cheng, W. R. Ewing and J. T. Groves, *Angew. Chem., Int. Ed.*, 2018, **57**, 1251–1255; (*c*) W. Liu, X. Huang and J. T. Groves, *Nature*, 2013, **8**, 2348–2354; (*d*) W. Liu, X. Huang, M. J. Cheng, R. J. Nielsen, W. A. Goddard III and J. T. Groves, *Science*, 2012, **337**, 1322–1325.
54 X. Huang, W. Liu, H. Ren, R. Neelamegam, J. M. Hooker and J. T. Groves, *J. Am. Chem. Soc.*, 2014, **136**, 6842–6845.
55 S. Bloom, C. R. Pitts, D. C. Miller, N. Haselton, M. G. Holl, E. Urheim and T. Lectka, *Angew. Chem., Int. Ed.*, 2012, **51**, 10580–10583.
56 Q. Wei, Y. Ma, L. Li, Q. Liu, Z. Liu and G. Liu, *Org. Lett.*, 2018, **20**, 7100–7103.
57 J. A. Buss, A. Vasilopoulos, D. L. Golden and S. S. Stahl, *Org. Lett.*, 2020, **22**, 5749–5752.
58 (*a*) H. Hintz, J. Bower, J. Tang, M. LaLama, C. Sevov and S. Zhang, *Chem. Catal.*, 2023, **3**, 100491; (*b*) J. K. Bower, A. D. Cypcar, B. Henriquez, S. C. E. Stieber and S. Zhang, *J. Am. Chem. Soc.*, 2020, **142**, 8514–8521.
59 J. Díaz, W. T. Or, J. T. Merrett, B. Xia and P. W. H. Chan, *Org. Lett.*, 2025, **27**, 3279–3283.
60 S. Bloom, C. R. Pitts, R. Woltornist, A. Griswold, M. G. Holl and T. Lectka, *Org. Lett.*, 2013, **15**, 1722–1724.
61 B. J. Groendyke, D. I. AbuSalim and S. P. Cook, *J. Am. Chem. Soc.*, 2016, **138**, 12771–12774.
62 H. Guan, S. Sun, Y. Mao, L. Chen, R. Lu, J. Huang and L. Liu, *Angew. Chem., Int. Ed.*, 2018, **57**, 11413–11417.
63 P. Guo, Y. Li, X. G. Zhang, J. F. Han, Y. Yu, J. Zhu and K. Y. Ye, *Org. Lett.*, 2020, **22**, 3601–3606.
64 J. B. Xia, Y. Ma and C. Chen, *Org. Chem. Front.*, 2014, **1**, 468–472.
65 P. Mondal, M. Lovisari, B. Twamley and A. R. McDonald, *Angew. Chem., Int. Ed.*, 2020, **59**, 13044–13050.
66 C. Panda, O. A. Nzekwue, L. M. Doyle, R. Gericke and A. R. McDonald, *JACS Au*, 2023, **3**, 919–928.
67 A. Das, B. Twamley, O. R. Kelly, C. Panda, P. Richardson and A. R. McDonald, *Angew. Chem., Int. Ed.*, 2025, **64**, e202421157.
68 (*a*) L. Hintermann and A. Togni, *Angew. Chem., Int. Ed.*, 2000, **39**, 4359–4362; (*b*) S. Piana, I. Devillers, A. Togni and U. Rothlisberger, *Angew. Chem., Int. Ed.*, 2002, **41**, 979–982.
69 R. Frantz, L. Hintermann, M. Perseghini, D. Broggini and A. Togni, *Org. Lett.*, 2003, **5**, 1709–1712.
70 H. Wack, A. E. Taggi, A. M. Hafex, W. J. Drury and T. Lectka, *J. Am. Chem. Soc.*, 2001, **123**, 1531–1532.
71 M. Marigo, N. Kumaragurubaran and K. A. Jorgensen, *Chem. – Eur. J.*, 2004, **10**, 2133–2137.
72 M. Frings and C. Bolm, *Eur. J. Org. Chem.*, 2009, 4085–4090.
73 K. Shibatomi, Y. Soga, A. Narayama, I. Fujisawa and S. Iwasa, *J. Am. Chem. Soc.*, 2012, **134**, 9836–9839.
74 D. S. Reddy, N. Shibata, T. Horikawa, S. Suzuki, S. Nakamura, T. Toru and M. Shiro, *Chem. – Asian J.*, 2009, **4**, 1411–1415.
75 J. Grover, A. T. Sebastian, S. Maiti, A. C. Bissember and D. Maiti, *Chem. Soc. Rev.*, 2025, **54**, 2006–2053.

 This journal is © The Royal Society of Chemistry 2026